

# Integrodifference equations in the presence of climate change: persistence criterion, travelling waves and inside dynamics

Mark A. Lewis · Nathan G. Marculis · Zhongwei Shen

*Dedicated to the memory of Professor Karl Peter Hadeler*

Received: date / Accepted: date

**Abstract** To understand the effects that the climate change has on the evolution of species as well as the genetic consequences, we analyze an integrodifference equation (IDE) models for a reproducing and dispersing population in a spatio-temporal heterogeneous environment described by a shifting climate envelope. Our analysis on the IDE focuses on the persistence criterion, travelling wave solutions, and the inside dynamics. First, the persistence criterion, characterizing the global dynamics of the IDE, is established in terms of the basic reproduction number. In the case of persistence, a unique travelling wave is found to govern the global dynamics. The effects of the size and the shifting speed of the climate envelope on the basic reproduction number, and hence, on the persistence criterion, are also investigated. In particular, the critical domain size and the critical shifting speed are found in certain cases. Numerical simulations are performed to complement the theoretical results. In the case of persistence, we separate the travelling wave and general solutions into spatially distinct neutral fractions to study the inside dynamics. It is shown that each neutral genetic fraction rearranges itself

---

This research was supported by a grant to MAL from the Natural Science and Engineering Research Council of Canada (Grant No. NET GP 434810-12) to the TRIA Network, with contributions from Alberta Agriculture and Forestry, Foothills Research Institute, Manitoba Conservation and Water Stewardship, Natural Resources Canada-Canadian Forest Service, Northwest Territories Environment and Natural Resources, Ontario Ministry of Natural Resources and Forestry, Saskatchewan Ministry of Environment, West Fraser and Weyerhaeuser. MAL is also grateful for support through NSERC Discovery and the Canada Research Chair Program. NGM acknowledges support from NSERC TRIA Network Collaborative Research Grant. ZS is supported by a start-up grant from the University of Alberta.

---

Mark A. Lewis

Department of Mathematical and Statistical Sciences, University of Alberta, Edmonton, AB T6G 2G1, Canada  
Department of Biological Sciences, University of Alberta, Edmonton, AB T6G 2G1, Canada  
E-mail: mark.lewis@ualberta.ca

Nathan G. Marculis

Department of Mathematical and Statistical Sciences, University of Alberta, Edmonton, AB T6G 2G1, Canada  
E-mail: marculis@ualberta.ca

Zhongwei Shen

Department of Mathematical and Statistical Sciences, University of Alberta, Edmonton, AB T6G 2G1, Canada  
E-mail: zhongwei@ualberta.ca

spatially so as to asymptotically achieve the profile of the travelling wave. To measure the genetic diversity of the population density we calculate the Shannon diversity index and related indices and use these to illustrate how diversity changes with underlying parameters.

**Keywords** Integrodifference equation · Persistence criterion · Travelling wave · Inside dynamics · Neutral genetic diversity · Diversity index

**Mathematics Subject Classification (2000)** 92D25 · 92D40 · 45G10 · 35C07 · 39A10

## 1 Introduction

Climate change is a serious threat to not only the survival of species but it is also known to affect the intraspecific genetic diversity [2]. The range of a species can be altered and shifted due to climate change [23]. In particular, climate change can alter the distribution of genetic variants in space and time [24]. Thus, it is important to understand how underlying biological processes linked with the effect of climate change alter the genetic distribution of a species.

Mathematically, reaction-diffusion equations of the form

$$u_t = u_{xx} + f(x - ct, u), \quad x \in \mathbb{R} \quad (1.1)$$

have been used to study the effect of climate change on the evolution of species as well as its genetic consequences, where  $c > 0$  is the shifting speed of the environment, and  $f$  is the growth rate function taking the form

$$f(x, u) = \begin{cases} ru \left(1 - \frac{u}{K}\right), & x \in (0, L), \\ -du, & x \in \mathbb{R} \setminus (0, L) \end{cases}$$

for some  $L > 0$  characterizing the size of the climate envelope [25, 3]. In the model (1.1), the climate envelope has size  $L$  and shifts to the right with speed  $c$ , and therefore, the growth rate function  $f$  introduces a special type of spatio-temporal heterogeneity. A fundamental question is whether the species can survive in the presence of climate change. In terms of (1.1), it is equivalent to ask about the long time behaviour of (non-negative) solutions of (1.1). In [3], the authors established the persistence criterion for (1.1) with more general growth rate functions of Fisher-KPP type. More precisely, they showed that solutions vanish as time elapses when the net reproduction number, defined to be the generalized principal eigenvalue of the operator  $u \mapsto u_{xx} + f_u(x, 0)u$ , is non-positive. When the net reproduction number crosses zero, there exists a unique travelling wave with speed  $c$  that attracts solutions. In the latter case, it is of great significance to understand the genetic structure of the travelling wave and general solutions of (1.1).

The genetic structure of solutions of (1.1), although generally very complex, can be understood for a simplified case where the wave is decomposed into a number of neutral fractions that differ only with respect to their initial spatial location within the wave front. The changes in the distribution and abundance of these neutral fractions as the wave progresses gives insight as to the effect of the nonlinear spatial dynamics on the genetic structure. The mathematical treatment of this problem, concerning the inside dynamics (see e.g. [7, 22, 1]), namely, the dynamics of neutral fractions of the travelling wave and general solutions, has been studied in [8].

When reaction-diffusion equations of the form (1.1) are used, it is implicitly assumed that the dispersal of the species follows the normal distribution with zero mean, which however is not the case for most species (see e.g. [13]). An alternative discrete-time continuous-space model often used in biological literature is the following integrodifference equation (IDE):

$$u_{n+1}(x) = \int_{\mathbb{R}} K(x-y)g(y-cn)f(u_n(y))dy, \quad x \in \mathbb{R}, \quad (1.2)$$

which prescribes the density  $u_{n+1}(x)$  in the  $(n+1)$ -th generation given the density in the  $n$ -th generation through two stages: a sedentary stage and a dispersal stage. An advantage of the IDE (1.2) over the reaction-diffusion equation (1.1) lies in the fact that (1.2) can be used to model the spatial spread of long-distance dispersers, while (1.1) is inappropriate in this situation.

In the IDE (1.2), the dispersal kernel  $K$  can be taken to be a Gaussian probability density function, a Laplace function, or, indeed, any other probability density function. Biologically, the dispersal kernel represents the probability that an individual moves from location  $y$  to location  $x$ . The function  $f$  is a density-dependent growth function. A typical example of  $f$  is the classical Beverton-Holt function [4]

$$f(u) = \frac{Ru}{1 + \frac{(R-1)u}{K_*}}, \quad u \geq 0 \quad (1.3)$$

where  $R > 0$  is the growth rate and  $K_* > 0$  is the carrying capacity. This growth function is commonly used by biologists because it is a simple function that exhibits negative density dependence. The function  $g$  is called the climate envelope or the climate envelope function. When  $g$  is the indicator function over  $\mathbb{R}$ , i.e.,  $g \equiv 1$  on  $\mathbb{R}$ , (1.2) becomes the classical and well-studied IDE:

$$u_{n+1}(x) = \int_{\mathbb{R}} K(x-y)f(u_n(y))dy, \quad x \in \mathbb{R}. \quad (1.4)$$

Population spread and travelling waves solutions have been widely studied for this model. The reader is referred to [31, 15, 16, 17, 18, 11, 9, 19] and references therein for the investigation of spreading speeds and travelling waves, and to [20] for the study of inside dynamics of (1.4). When  $g$  is the indicator function over the interval  $[-\frac{L}{2}, \frac{L}{2}]$ , i.e.,  $g(x) = 1_{[-\frac{L}{2}, \frac{L}{2}]}(x)$ , we obtain a particular form of (1.2) that has been previously studied in [33]. Their work focused on determining the critical speed for extinction and the role that the dispersal and growth play in persistence.

To summarize, the purpose of this endeavour is to understand the effects that climate change has on the dynamics of the IDE (1.2) with the focus on two fundamental aspects: persistence criterion and inside dynamics. To perform the mathematical analysis of (1.2), we make the following assumptions throughout the paper.

**(H)** We make the following assumptions.

- (1) The dispersal kernel  $K : \mathbb{R} \rightarrow (0, \infty)$  is a continuous probability density function.
- (2) The growth function  $f : [0, \infty) \rightarrow [0, \infty)$  is bounded, Lipschitz continuous and increasing, and satisfies the following conditions:

$$f(0) = 0, \quad f'(0) > 1 \quad \text{and} \quad \frac{f(u)}{u} < \frac{f(v)}{v} \quad \text{for } u > v > 0,$$

where  $f'(0)$  denotes the right-derivative of  $f$  at 0.

- (3) The climate envelope  $g : \mathbb{R} \rightarrow [0, \infty)$  has an upper bound of 1 and is compactly supported. Let  $I := \text{supp}(g)$  be a nonempty interval.
- (4) The number  $c > 0$  is the shifting speed of the environment or the climate envelope.

As  $K$  is a probability density function,  $\int_{\mathbb{R}} K(x) dx = 1$  implies  $K(x) \rightarrow 0$  as  $|x| \rightarrow \infty$ , but we impose no condition on how fast  $K(x)$  decays as  $|x| \rightarrow \infty$ . In particular, the so-called fat-tailed kernels are allowed. A typical example satisfies the assumptions on the growth function  $f$  is the Beverton-Holt function (1.3) with  $R > 1$ . Our assumptions on the growth function excludes any Allee effect.

For the purpose of stating main results and performing analysis in this paper we define the following spaces for convenience. Recall that  $I$  is a compact interval.

$$\begin{aligned} C(I) &= \{u : I \rightarrow \mathbb{R} : u \text{ is continuous}\}, \\ C_+(I) &= \{u \in C(I) : u(x) \geq 0, x \in I\}, \\ C_{++}(I) &= \{u \in C(I) : u(x) > 0, x \in I\} = \left\{u \in C(I) : \min_{x \in I} u(x) > 0\right\}. \end{aligned}$$

The space  $C(I)$  is equipped with the max norm  $\|\cdot\|_{C(I)}$ . Clearly,  $C_+(I)$  is the positive cone of  $C(I)$  and  $C_{++}(I)$  is the interior of  $C_+(I)$ . Also, we define

$$\begin{aligned} C(\mathbb{R}) &= \{u : \mathbb{R} \rightarrow \mathbb{R} : u \text{ is continuous}\}, \\ C_+(\mathbb{R}) &= \{u \in C(\mathbb{R}) : u(x) \geq 0, x \in \mathbb{R}\}. \end{aligned}$$

Main results obtained in the present paper are roughly summarized in the following theorem. We denote by  $\{u_n\}_{n \in \mathbb{Z}_0}$  an arbitrary solution of (1.2) with initial data  $u_0 \in C_+(\mathbb{R})$  being non-zero on  $I$ .

**Theorem 1.1** *The following statements hold.*

- (1) (*Persistence criterion*) Let  $R_0$  be the spectral radius of the operator  $\mathcal{F}_0 : C(I) \rightarrow C(I)$  defined by

$$\mathcal{F}_0[w](x) = f'(0) \int_I K(x - y + c)g(y)w(y)dy, \quad x \in I, \quad w \in C(I).$$

Then,

- if  $R_0 \leq 1$ ,  $u_n(x) \rightarrow 0$  uniformly in  $x \in \mathbb{R}$  as  $n \rightarrow \infty$ ;
  - if  $R_0 > 1$ , then (1.2) admits a unique travelling wave  $\{w^*(\cdot - cn)\}_{n \in \mathbb{Z}}$  such that  $u_n(x + cn) \rightarrow w^*(x)$  uniformly in  $x \in \mathbb{R}$  as  $n \rightarrow \infty$ .
- (2) (*Effects of the size of the climate envelope*) Assume  $g(x) = 1_{[-\frac{L}{2}, \frac{L}{2}]}(x)$  for  $x \in \mathbb{R}$  and  $L > 0$ , and write  $R_0$  as  $R_0(L)$ . Then, the function  $L \mapsto R_0(L)$  is bounded, continuous and increasing on  $(0, \infty)$ , and satisfies  $\lim_{L \rightarrow 0^+} R_0(L) = 0$ . Set

$$R_0(\infty) := \lim_{L \rightarrow \infty} R_0(L).$$

Then,

- $R_0(\infty) \leq 1$  implies that  $R_0(L) < 1$  for all  $L > 0$ ;
- $R_0(\infty) > 1$  implies the existence some  $L_* > 0$  such that  $R_0(L) < 1$  for  $L \in (0, L_*)$  and  $R_0(L) > 1$  for  $L > L_*$ .

- (3) *(Effects of the shifting speed of the climate envelope)* Assume  $K$  is a Gaussian probability density function with mean  $\mu \in \mathbb{R}$  and variance  $\sigma^2 > 0$ , and  $K_0$  is a Gaussian probability density function with mean 0 and variance  $\sigma^2$ . Then,

$$R_0 = e^{-\frac{(c-\mu)^2}{2\sigma^2}} r(\mathcal{F}_{00}),$$

where  $r(\mathcal{F}_{00})$  is the spectral radius of the operator  $\mathcal{F}_{00} : C(I) \rightarrow C(I)$  defined by

$$\mathcal{F}_{00}[w](x) = f'(0) \int_I K_0(x-y+c)g(y)w(y)dy, \quad x \in I, \quad w \in C(I).$$

- (4) *(Inside dynamics)* Suppose  $R_0 > 1$ . Let  $v_0 \in C_+(\mathbb{R})$  be a portion of  $u_0$ , that is,  $0 \not\leq v_0 \leq u_0$ . Consider the solution  $\{v_n\}_{n \in \mathbb{N}_0}$  of

$$v_{n+1}(x) = \int_{\mathbb{R}} K(x-y)g(y-cn)\frac{f(u_n(y))}{u_n(y)}v_n(y)dy, \quad x \in \mathbb{R}$$

with initial condition  $v_0$ . Then there exists a constant  $p := p(v_0) \in [0, 1]$  such that

$$v_n(x+cn) \rightarrow pw^*(x) \quad \text{uniformly in } x \in \mathbb{R} \text{ as } n \rightarrow \infty.$$

Moreover, if, in addition,  $v_0 \not\equiv 0$  on  $I$ , then  $p > 0$ . Suppose, in addition, that  $u_0 = w^*$  and  $K$  is a Gaussian probability density function with mean  $\mu \in \mathbb{R}$  and variance  $\sigma^2 > 0$ , then

$$p = \frac{\int_I v_0(x)g(x)f(w^*(x))e^{\frac{2(c-\mu)x}{\sigma^2}} dx}{\int_I w^*(x)g(x)f(w^*(x))e^{\frac{2(c-\mu)x}{\sigma^2}} dx}.$$

In our work, we begin by studying the persistence criterion for (1.2). The main persistence results are laid out in Section 2. The effects of the size and the shifting speed of the climate envelope on persistence of the population are considered in Subsections 2.3 and 2.4, respectively. In Subsection 2.5, numerical simulations are provided to increase the clarity of theoretical results. We continue our analysis of (1.2) by investigating the inside dynamics of (1.2). A formulation for the inside dynamics of (1.2) is presented in Section 3. The analysis of the inside dynamics follows in Subsections 3.1 and 3.2. Subsection 3.3 finishes with a few numerical simulations exemplifying the theoretical results proven earlier in the section. This paper concludes with a discussion of the theoretical and numerical results in Section 4.

## 2 Persistence criterion

The purpose of this section is to study the persistence criterion for (1.2), namely, the criterion classifying the global dynamics of (1.2). In Subsection 2.1, we derive an equivalent problem and establish the persistence criterion for the equivalent problem. In Subsection 2.2, we study the persistence criterion for (1.2). In Subsections 2.3 and 2.4, we investigate the effects of the size of the climate envelope and the shifting speed of the environment, respectively, on the persistence criterion. In Subsection 2.5, we provide some numerical simulations to support our theoretical results.

## 2.1 Equivalent formalism and analysis

A fundamental question concerning (1.2) is whether a species, whose dynamics are modelled by (1.2), can survive or not in the long run. In the presence of the climate change, this question can be rephrased as whether the species can keep up with the shift of the environment. This suggests to look for travelling waves of (1.2) with speed  $c$ , the shifting speed of the climate envelope, and to study their properties, especially, the stability.

**Definition 2.1** *An entire solution  $\{u_n\}_{n \in \mathbb{Z}}$  of (1.2) is called a travelling wave or a travelling wave solution if there is a measurable function  $w : \mathbb{R} \rightarrow [0, \infty)$  with  $w \geq 0$  such that*

$$u_n(x) = w(x - cn), \quad x \in \mathbb{R}, \quad n \in \mathbb{Z},$$

where  $c$  is the same as in (1.2). The function  $w$  is called a profile or a profile function.

Suppose  $\{w(\cdot - cn)\}_{n \in \mathbb{Z}}$  is a travelling wave of (1.2). Inserting it into (1.2) results in

$$\begin{aligned} w(x - c(n+1)) &= \int_{\mathbb{R}} K(x-y)g(y-cn)f(w(y-cn))dy \\ &= \int_{\mathbb{R}} K(x-cn-y)g(y)f(w(y))dy, \quad x \in \mathbb{R}, \quad n \in \mathbb{Z}. \end{aligned}$$

The change of variable  $x \rightarrow x + c(n+1)$  gives

$$w(x) = \int_{\mathbb{R}} K(x-y+c)g(y)f(w(y))dy, \quad x \in \mathbb{R}, \quad (2.1)$$

which is the stationary equation for the profile  $w$ . Since  $g$  is compactly supported, solving (2.1) for  $w$  is equivalent to solving the following equation

$$w(x) = \int_I K(x-y+c)g(y)f(w(y))dy, \quad x \in I,$$

for  $w$  defined on  $I$ . This suggests to consider the following equation:

$$w_{n+1}(x) = \mathcal{F}[w_n](x), \quad x \in I, \quad (2.2)$$

where the map  $\mathcal{F}$  is defined by

$$\mathcal{F}[w](x) = \int_I K(x-y+c)g(y)f(w(y))dy, \quad x \in I.$$

Then, finding travelling waves of (1.2) is equivalent to finding non-trivial stationary solutions of (2.2). For clarity, we give the following definition.

**Definition 2.2** *A measurable function  $w : I \rightarrow [0, \infty)$  is called a stationary solution of (2.2) if it satisfies  $w = \mathcal{F}[w]$ . A stationary solution  $w$  of (2.2) is called positive if  $w \not\equiv 0$ .*

To study the existence and non-existence of positive stationary solutions of (2.2), we consider the linear operator  $\mathcal{F}_0$  defined by

$$\mathcal{F}_0[w](x) = r_0 \int_I K(x - y + c)g(y)w(y)dy, \quad x \in I,$$

where  $r_0 = f'(0)$ . It is the linearization of  $\mathcal{F}$  at  $w \equiv 0$ .

Clearly,  $\mathcal{F}_0$  is a bounded linear operator on  $C(I)$ , and it is strongly positive, namely,  $\mathcal{F}_0[C_+(I) \setminus \{0\}] \subset C_{++}(I)$ . Moreover, it is easy to check that  $\mathcal{F}_0$  is compact. Therefore, we can apply the Krein-Rutman theorem (see e.g. [12,30]) to  $\mathcal{F}_0$  to conclude that the spectral radius of  $\mathcal{F}_0$ , denoted by  $r(\mathcal{F}_0)$ , is an algebraically simple eigenvalue with an associated eigenfunction  $\phi_0 \in C_{++}(I)$ . Also, if  $\lambda \in \sigma(\mathcal{F}_0)$ , the spectrum of  $\mathcal{F}_0$ , then either  $\lambda = r(\mathcal{F}_0)$  or  $|\lambda| < r(\mathcal{F}_0)$ . In addition, if  $\lambda$  is an eigenvalue of  $\mathcal{F}_0$  with an associated eigenfunction in  $C_+(I) \setminus \{0\}$ , then  $\lambda = r(\mathcal{F}_0)$ . Set

$$R_0 := r(\mathcal{F}_0).$$

Clearly,  $R_0 > 0$ . The number  $R_0$  is often referred to as the *basic reproduction number*. By the assumptions on  $K$  and  $g$ , there holds  $R_0 \leq \|\mathcal{F}_0\| \leq r_0$ .

The main result in this subsection is summarized in the following theorem.

**Theorem 2.3** *The following statements hold.*

- (1) *If  $R_0 \leq 1$ , then 0 is the unique stationary solution of (2.2). If  $R_0 > 1$ , there exists a unique positive stationary solution  $w_*$  of (2.2). Moreover,  $\sup_I w_* \leq \sup_{u \in [0, \infty)} f(u)$ .*
- (2) *Let  $\{w_n\}_n$  be a solution of (2.2) with initial condition  $w_0 \in C_+(I) \setminus \{0\}$ . Then the following statements hold.*
  - (i) *If  $R_0 \leq 1$ , then  $w_n \rightarrow 0$  in  $C(I)$  as  $n \rightarrow \infty$ .*
  - (ii) *If  $R_0 > 1$ , then  $w_n \rightarrow w_*$  in  $C(I)$  as  $n \rightarrow \infty$ .*

We point out that the proof of Theorem 2.3 falls into the scope of abstract results established in [32]. For self-completeness, we provide the elementary proof of Theorem 2.3 in Appendix A.

## 2.2 Travelling waves and global dynamics

So far, we have been focusing on the equivalent problem (2.2). Let us now go back to the IDE (1.2). We are interested in travelling waves of (1.2) (see Definition 2.1). By the analysis at the beginning of Subsection 2.1, the profile function  $w$  for a travelling wave of (1.2) satisfies (2.1), and therefore, the restriction of  $w$  on  $I$  completely determines  $w$ . By Theorem 2.3, we obtain the following result concerning the existence and non-existence of travelling waves, as well as the global dynamics of (1.2). Recall that  $w_*$  is the unique positive stationary solution of (2.2) in the case  $R_0 > 1$ .

**Theorem 2.4** *The following statements hold.*

- (1) If  $R_0 \leq 1$ , then (1.2) admits no travelling wave. If  $R_0 > 1$ , then (1.2) admits a unique travelling wave  $\{w^*(\cdot - cn)\}_{n \in \mathbb{Z}}$ , where

$$w^*(x) = \int_I K(x - y + c)g(y)f(w_*(y))dy, \quad x \in \mathbb{R}. \quad (2.3)$$

In particular,  $w^* \in C_+(\mathbb{R}) \setminus \{0\}$  and satisfies  $w^*(x) \rightarrow 0$  as  $|x| \rightarrow \infty$ .

- (2) Let  $\{u_n\}_n$  be a solution of (1.2) with initial condition  $u_0 \in C_+(\mathbb{R})$  being non-zero on  $I$ . Then the following statements hold.
- (i) If  $R_0 \leq 1$ , then  $u_n(x) \rightarrow 0$  uniformly in  $x \in \mathbb{R}$  as  $n \rightarrow \infty$ .
  - (ii) If  $R_0 > 1$ , then  $u_n(x) \rightarrow w^*(x - cn)$  uniformly in  $x \in \mathbb{R}$  as  $n \rightarrow \infty$ .

*Proof* (1) In the case of  $R_0 \leq 1$ , if there is a travelling wave of (1.2), then (2.2) admits a positive stationary solution, which contradicts to Theorem 2.3.

If  $R_0 > 1$ , then it is easy to see that  $w^*$  is a profile for a travelling wave and satisfies required properties. The uniqueness of travelling waves in this case follows readily as the existence of another travelling wave gives a second positive stationary solution of (2.2), which contradicts Theorem 2.3.

(2) Note that the solution  $\{u_n\}_n$  satisfies

$$u_{n+1}(x + c(n + 1)) = \int_I K(x - y + c)g(y)f(u_n(y + cn))dy, \quad x \in \mathbb{R}.$$

It follows from Theorem 2.3(2) that the sequence  $\{u_n(\cdot + cn)\}_n$  restricted to  $I$  converges in  $C(I)$  to 0 when  $R_0 \leq 1$  and to  $w_*$  when  $R_0 > 1$  as  $n \rightarrow \infty$ .

Now, if  $R_0 \leq 1$ , then

$$\begin{aligned} \sup_{x \in \mathbb{R}} u_{n+1}(x + c(n + 1)) &\leq \sup_{x \in \mathbb{R}} \int_I K(x - y + c)g(y)f(u_n(y + cn))dy \\ &\leq \left[ \sup_{x \in \mathbb{R}} \int_I K(x - y + c)g(y)dy \right] f'(0) \|u_n(\cdot + cn)\|_{C(I)} \\ &\rightarrow 0 \quad n \rightarrow \infty. \end{aligned}$$

If  $R_0 > 1$ , then

$$\begin{aligned} \sup_{x \in \mathbb{R}} |u_{n+1}(x + c(n + 1)) - w^*(x)| &\leq \sup_{x \in \mathbb{R}} \int_I K(x - y + c)g(y)|f(u_n(y + cn)) - f(w_*(y))|dy \\ &\leq \left[ \sup_{x \in \mathbb{R}} \int_I K(x - y + c)g(y)dy \right] Lip(f) \|u_n(\cdot + cn) - w_*\|_{C(I)} \\ &\rightarrow 0 \quad n \rightarrow \infty, \end{aligned}$$

where  $Lip(f)$  is the Lipschitz constant of  $f$ .

This completes the proof.

We end this subsection by making some remarks about Theorem 2.4.

**Remark 2.5** By (2.3) and the equation satisfied by  $w_*$ , we have  $w^*(x) = w_*(x)$  for  $x \in I$ . In Theorem 2.4 (2), the value of the initial data  $u_0$  on  $\mathbb{R} \setminus I$  is irrelevant as the climate envelope  $g$  is supported on  $I$ . In particular, if  $u_0 \equiv 0$  on  $I$ , then  $u_n \equiv 0$  for all  $n \geq 1$ . Moreover, the conclusions of Theorem 2.4 (2) are valid for measurable initial data, since  $u_1$  is always continuous and can be treated as the new initial data. This provides theoretical supports for our simulations done later, where initial data is chosen to be discontinuous functions such as indicator functions over intervals.

A full version of Theorem 2.4 (2) reads as follows: Let  $\{u_n\}_n$  be a solution of (1.2) with initial condition  $u_0 : \mathbb{R} \rightarrow [0, \infty)$  being measurable. If  $u_0 = 0$  a.e. on  $I$ , then  $u_n \equiv 0$  for all  $n \geq 1$ . Otherwise, the following statements hold.

- (i) If  $R_0 \leq 1$ , then  $u_n(x) \rightarrow 0$  uniformly in  $x \in \mathbb{R}$  as  $n \rightarrow \infty$ .
- (ii) If  $R_0 > 1$ , then  $u_n(x) \rightarrow w^*(x - cn)$  uniformly in  $x \in \mathbb{R}$  as  $n \rightarrow \infty$ .

### 2.3 Effects of the size of the climate envelope

In this subsection, we assume

$$g(x) = g_L(x) = 1_{[-\frac{L}{2}, \frac{L}{2}]}(x), \quad x \in \mathbb{R}, \quad (2.4)$$

and study the influence of  $L$  on the basic reproduction number, and hence, on the persistence criterion. To indicate the  $L$ -dependence, the operator  $\mathcal{F}_0$  is written as  $\mathcal{F}_{0,L}$ :

$$\mathcal{F}_{0,L}[w](x) := r_0 \int_{I_L} K(x - y + c)w(y)dy, \quad x \in I_L := \left[-\frac{L}{2}, \frac{L}{2}\right],$$

and the basic reproduction number  $R_0$  is written as  $R_0(L)$ . We prove the following result.

**Theorem 2.6** Let  $g = g_L$  be as in (2.4). Then the following statements hold.

- (1) The function  $L \mapsto R_0(L)$  is continuous and increasing on  $(0, \infty)$ .
- (2) There holds the limit

$$\lim_{L \rightarrow 0^+} R_0(L) = 0.$$

- (3) Set

$$R_0(\infty) := \lim_{L \rightarrow \infty} R_0(L).$$

Then,

- (i) if  $R_0(\infty) \leq 1$ , then  $R_0(L) < 1$  for all  $L > 0$ ;
- (ii) if  $R_0(\infty) > 1$ , then there exists  $L_* > 0$  such that  $R_0(L) < 1$  for  $L \in (0, L_*)$  and  $R_0(L) > 1$  for  $L > L_*$ .

*Proof* (1) We first prove the monotonicity. Let  $0 < L_1 < L_2$ . For  $i = 1, 2$ , let  $\phi_{L_i} \in C_{++}(I_{L_i})$  be an eigenfunction of  $\mathcal{F}_{0,L_i}$  associated to  $R_0(L_i)$ . We may choose  $\phi_{L_1}$  and  $\phi_{L_2}$  so that

$$\phi_{L_1}(x) \leq \phi_{L_2}(x), \quad x \in I_{L_1} \quad (2.5)$$

and

$$\phi_{L_1}(x_0) = \phi_{L_2}(x_0) \text{ for some } x_0 \in I_{L_1}. \quad (2.6)$$

It follows from (2.5) that

$$\begin{aligned} R_0(L_1)\phi_{L_1}(x_0) &= \mathcal{F}_{0,L_1}[\phi_{L_1}](x_0) \\ &= r_0 \int_{I_{L_1}} K(x_0 - y + c)\phi_{L_1}(y)dy \\ &\leq r_0 \int_{I_{L_1}} K(x_0 - y + c)\phi_{L_2}(y)dy \\ &< r_0 \int_{I_{L_2}} K(x_0 - y + c)\phi_{L_2}(y)dy \\ &= \mathcal{F}_{0,L_2}[\phi_{L_2}](x_0) \\ &= R_0(L_2)\phi_{L_2}(x_0). \end{aligned}$$

Applying (2.6), we conclude  $R_0(L_1) < R_0(L_2)$ . This proves the monotonicity of the function  $L \mapsto R_0(L)$ .

Next, we prove the continuity. Fix any  $L_0 > 0$  and  $0 < \epsilon_0 \ll 1$ , and let  $\{L_n\}_n \subset (L_0 - \epsilon_0, L_0 + \epsilon_0)$  be such that  $L_n \rightarrow L_0$  as  $n \rightarrow \infty$ . By the monotonicity proven above,  $\{R_0(L_n)\}_n \subset (R_0(L_0 - \epsilon_0), R_0(L_0 + \epsilon_0))$ . For each  $n$ , let  $\phi_n \in C_{++}(I_{L_n})$  be an eigenfunction of  $\mathcal{F}_{0,L_n}$  associated to  $R_0(L_n)$  and satisfy the normalization

$$\phi_n(0) = 1, \quad \forall n. \quad (2.7)$$

We claim that

$$M := \sup_n \|\phi_n\|_{C(I_{L_n})} < \infty. \quad (2.8)$$

In fact, from the equation  $\mathcal{F}_{0,L_n}[\phi_n] = R_0(L_n)\phi_n$ , we deduce

$$R_0(L_n) = R_0(L_n)\phi_n(0) = r_0 \int_{I_{L_n}} K(-y + c)\phi_n(y)dy \geq r_0 \left[ \min_{y \in I_{L_n}} K(-y + c) \right] \int_{I_{L_n}} \phi_n(y)dy.$$

Since clearly  $\tilde{M} := \inf_n \min_{y \in I_{L_n}} K(-y + c) > 0$ , we find

$$\sup_n \int_{I_{L_n}} \phi_n(y)dy \leq \sup_n \frac{R_0(L_n)}{r_0 \tilde{M}} \leq \frac{R_0(L_0 + \epsilon_0)}{r_0 \tilde{M}}. \quad (2.9)$$

It then follows that

$$\begin{aligned} R_0(L_n)\|\phi_n\|_{C(I_{L_n})} &= r_0 \max_{x \in I_{L_n}} \int_{I_{L_n}} K(x - y + c)\phi_n(y)dy \\ &\leq r_0 \left[ \max_{x \in I_{L_n}} \max_{y \in I_{L_n}} K(x - y + c) \right] \int_{I_{L_n}} \phi_n(y)dy. \end{aligned}$$

Since

$$\sup_n \max_{x \in I_{L_n}} \max_{y \in I_{L_n}} K(x - y + c) < \infty,$$

we conclude (2.8) from  $R_0(L_n) \geq R_0(L_0 - \epsilon_0)$  for each  $n$  and (2.9).

We further claim that  $\{\phi_n\}_n$  are equi-continuous in the sense that

$$\begin{aligned} \forall \epsilon > 0, \text{ there exists } \delta = \delta(\epsilon) > 0 \text{ such that} \\ |\phi_n(x) - \phi_n(y)| < \epsilon \text{ whenever } x, y \in I_{L_n}, |x - y| < \delta \text{ for all } n. \end{aligned} \quad (2.10)$$

Indeed, for  $x, y \in I_{L_n}$ , there holds

$$|\phi_n(x) - \phi_n(y)| \leq r_0 \int_{I_{L_n}} |K(x-z+c) - K(y-z+c)| \phi_n(z) dz \leq r_0 M \int_{I_{L_n}} |K(x-z+c) - K(y-z+c)| dz,$$

which leads to (2.10).

Now, by (2.8), (2.10) and the Arzelà-Ascoli theorem, there exist a subsequence of  $\{\phi_n\}_n$ , denoted by  $\{\phi_{n_k}\}_k$ , and a function  $\phi_\infty \in C(I_{L_0}^\circ)$  (where  $I_{L_0}^\circ$  is the interior of  $I_{L_0}$ ) with  $\phi_\infty \geq 0$  such that  $\phi_{n_k}(x)$  converges to  $\phi_\infty(x)$  locally uniformly in  $x \in I_{L_0}^\circ$  as  $k \rightarrow \infty$ . Moreover, the normalization (2.7) ensures that  $\phi_\infty(0) = 1$  and (2.8) implies that  $\phi_\infty$  is bounded on  $I_{L_0}^\circ$ . Also, the equations satisfied by  $\{\phi_n\}_n$  give

$$\tilde{R}_0(L_0) \phi_\infty(x) = r_0 \int_{I_{L_0}} K(x-y+c) \phi_\infty(y) dy, \quad x \in I_{L_0}^\circ, \quad (2.11)$$

where  $\tilde{R}_0(L_0) := \lim_{k \rightarrow \infty} R_0(L_{n_k})$ , which is well-defined by choosing a further subsequence if necessary. Using (2.11), we can first extend  $\phi_\infty$  to be defined as a continuous function, still denoted by  $\phi_\infty$ , on  $I_{L_0}$  so that (2.11) is true for all  $x \in I_{L_0}$ . Then, it is easy to see that  $\phi_\infty \in C_{++}(I_{L_0})$ , which together with the Krein-Rutman theorem yield  $\tilde{R}_0(L_0) = R_0(L_0)$ . Hence,  $\lim_{k \rightarrow \infty} R_0(L_{n_k}) = R_0(L_0)$ .

So far, we have shown that for any sequence  $\{L_n\}_n$  such that  $L_n \rightarrow L_0$  as  $n \rightarrow \infty$ , there is a subsequence  $\{L_{n_k}\}_k \subset \{L_n\}_n$  such that  $R_0(L_{n_k}) \rightarrow R_0(L_0)$  as  $k \rightarrow \infty$ . From this, we conclude the continuity of the function  $L \mapsto R_0(L)$  at  $L = L_0$ . Since  $L_0$  is arbitrary, the continuity of  $L \mapsto R_0(L)$  follows.

(2) We see that

$$\|\mathcal{F}_{0,L}[w]\|_{C(I_L)} \leq r_0 \left[ \max_{x \in I_L} \int_{I_L} K(x-y+c) dy \right] \|w\|_{C(I_L)},$$

which implies that

$$R_0(L) \leq \|\mathcal{F}_{0,L}\| \leq r_0 \left[ \max_{x \in I_L} \int_{I_L} K(x-y+c) dy \right] \leq r_0 \int_{-L+c}^{L+c} K(y) dy \rightarrow 0 \quad \text{as } L \rightarrow 0^+.$$

Hence,  $\lim_{L \rightarrow 0^+} R_0(L) = 0$ .

(3) It is a simple consequence of (1) and (2).

This completes the proof.

Next, we calculate  $R_0(\infty)$  in the case of  $K$  being a Gaussian probability density function, namely,

$$K(x) = \frac{1}{\sqrt{2\pi\sigma}} e^{-\frac{(x-\mu)^2}{2\sigma^2}}, \quad x \in \mathbb{R} \quad (2.12)$$

for some  $\sigma > 0$  and  $\mu \in \mathbb{R}$ . Let

$$K_0(x) = \frac{1}{\sqrt{2\pi\sigma}} e^{-\frac{x^2}{2\sigma^2}}, \quad x \in \mathbb{R}. \quad (2.13)$$

**Theorem 2.7** *Let  $g = g_L$  be as in (2.4) and  $K$  be as in (2.12). Then*

$$R_0(\infty) = e^{-\frac{(c-\mu)^2}{2\sigma^2}} r_0.$$

*Proof* We need the following result (to be established in Theorem 2.8 below):

$$R_0(L) = e^{-\frac{(c-\mu)^2}{2\sigma^2}} r_0 r(\mathcal{F}_L), \quad (2.14)$$

where  $r(\mathcal{F}_L)$  is the spectral radius of the operator  $\mathcal{F}_L : C(I) \rightarrow C(I)$  defined by

$$\mathcal{F}_L[w](x) = \int_{I_L} K_0(x-y)w(y)dy, \quad x \in I_L.$$

Using (2.14), we only need to show that

$$\lim_{L \rightarrow \infty} r(\mathcal{F}_L) = 1. \quad (2.15)$$

To prove (2.15), we first present the following classical variational formula for  $r(\mathcal{F}_L)$ , that is,

$$r(\mathcal{F}_L) = \sup_{w \in L^2(I_L) \setminus \{0\}} \frac{\langle \mathcal{F}_L[w], w \rangle_{L^2(I_L)}}{\|w\|_{L^2(I_L)}^2} = \sup_{w \in L^2(I_L) \setminus \{0\}} \frac{\int_{I_L} \int_{I_L} K_0(x-y)w(y)w(x)dydx}{\int_{I_L} w(x)^2 dx}.$$

We refer the reader to [6] for the proof, which requires the self-adjointness of  $\mathcal{F}_L$ .

Next, we choose  $w \equiv 1$  on  $I_L$  as a test function to find

$$r(\mathcal{F}_L) \geq \frac{1}{L} \int_{-\frac{L}{2}}^{\frac{L}{2}} \int_{-\frac{L}{2}}^{\frac{L}{2}} K_0(x-y)dydx. \quad (2.16)$$

We claim that for each  $\epsilon > 0$  there exists  $L_\epsilon > 0$  such that

$$\int_{-\frac{L}{2}}^{\frac{L}{2}} \int_{-\frac{L}{2}}^{\frac{L}{2}} K_0(x-y)dydx \geq (1-\epsilon)(L-L_\epsilon), \quad \forall L > L_\epsilon. \quad (2.17)$$

In fact, for each  $\epsilon > 0$  there exists  $L_\epsilon > 0$  such that  $\int_{-\frac{L_\epsilon}{2}}^{\frac{L_\epsilon}{2}} K_0(x)dx \geq 1-\epsilon$ . Now, for  $L > L_\epsilon$ , we have for each  $x \in [-\frac{L}{2} + \frac{L_\epsilon}{2}, \frac{L}{2} - \frac{L_\epsilon}{2}]$

$$\int_{-\frac{L}{2}}^{\frac{L}{2}} K_0(x-y)dy \geq \int_{-\frac{L_\epsilon}{2}+x}^{\frac{L_\epsilon}{2}+x} K_0(x-y)dy \geq 1-\epsilon.$$

It then follows that

$$\int_{-\frac{L}{2}}^{\frac{L}{2}} \int_{-\frac{L}{2}}^{\frac{L}{2}} K_0(x-y)dydx \geq \int_{-\frac{L}{2}}^{\frac{L}{2}} (1-\epsilon)1_{[-\frac{L}{2}+\frac{L_\epsilon}{2}, \frac{L}{2}-\frac{L_\epsilon}{2}]}(x)dx = (1-\epsilon)(L-L_\epsilon).$$

This proves (2.17).

Finally, by (2.16) and (2.17), we find that for each  $\epsilon > 0$ , there exists  $L_\epsilon > 0$  such that

$$r(\mathcal{F}_L) \geq (1-\epsilon)\frac{L-L_\epsilon}{L}, \quad L > L_\epsilon.$$

Setting  $L \rightarrow \infty$  in the above inequality, we find for each  $\epsilon > 0$ ,

$$\liminf_{L \rightarrow \infty} r(\mathcal{F}_L) \geq (1 - \epsilon).$$

Thus,  $\liminf_{L \rightarrow \infty} r(\mathcal{F}_L) \geq 1$ . As clearly  $r(\mathcal{F}_L) \leq 1$  for all  $L > 0$ , we arrive at (2.15) and hence complete the proof.

#### 2.4 Effects of the shifting speed

In this subsection, we investigate the influence of the shifting speed  $c$  of the environment on the basic reproduction number, and hence, on the persistence criterion, in the case of  $K$  being a Gaussian probability density function as in (2.12). We prove the following result.

**Theorem 2.8** *Let  $K$  be as in (2.12) and  $K_0$  be as in (2.13). Then*

$$R_0 = e^{-\frac{(c-\mu)^2}{2\sigma^2}} r(\mathcal{F}_{00}),$$

where  $r(\mathcal{F}_{00})$  is the spectral radius of the operator  $\mathcal{F}_{00} : C(I) \rightarrow C(I)$  defined by

$$\mathcal{F}_{00}[w](x) = r_0 \int_I K_0(x-y)g(y)w(y)dy, \quad x \in I.$$

In particular, the following statements hold.

- (1) If  $r(\mathcal{F}_{00}) \leq 1$ , then  $R_0 \leq 1$  for all  $c > 0$ .
- (2) If  $r(\mathcal{F}_{00}) > 1$ ,  $\mu \leq 0$  and  $e^{-\frac{\mu^2}{2\sigma^2}} r(\mathcal{F}_{00}) \leq 1$ , then  $R_0 \leq 1$  for all  $c > 0$ .
- (3) If  $r(\mathcal{F}_{00}) > 1$ ,  $\mu \leq 0$  and  $e^{-\frac{\mu^2}{2\sigma^2}} r(\mathcal{F}_{00}) > 1$ , then there exists  $c_* > 0$  such that  $R_0 > 1$  for  $c \in (0, c_*)$  and  $R_0 \leq 1$  for  $c \geq c_*$ .
- (4) If  $r(\mathcal{F}_{00}) > 1$  and  $\mu > 0$ , then there exist  $0 \leq c_*^1 < c_*^2 < \infty$  such that  $R_0 > 1$  for  $c \in (c_*^1, c_*^2)$  and  $R_0 \leq 1$  for  $c \in (0, c_*^1] \cup [c_*^2, \infty)$ .

*Proof* Let  $\phi_0 \in C_{++}(I)$  be the eigenfunction of  $\mathcal{F}_0$  associated to the eigenvalue  $R_0$ . Then there holds the identity

$$\begin{aligned} R_0 \phi_0(x) &= r_0 \int_I K(x-y+c)g(y)\phi_0(y)dy \\ &= r_0 \int_I \frac{1}{\sqrt{2\pi}\sigma} e^{-\frac{(x-y+c-\mu)^2}{2\sigma^2}} g(y)\phi_0(y)dy \\ &= r_0 e^{-\frac{(c-\mu)x}{\sigma^2}} e^{-\frac{(c-\mu)^2}{2\sigma^2}} \int_I K_0(x-y)g(y) \left[ e^{\frac{(c-\mu)y}{\sigma^2}} \phi_0(y) \right] dy, \quad x \in I. \end{aligned}$$

Multiplying the above equation by  $e^{\frac{(c-\mu)x}{\sigma^2}} e^{\frac{(c-\mu)^2}{2\sigma^2}}$ , we find

$$R_0 e^{\frac{(c-\mu)^2}{2\sigma^2}} e^{\frac{(c-\mu)x}{\sigma^2}} \phi_0(x) = r_0 \int_I K_0(x-y)g(y) \left[ e^{\frac{(c-\mu)y}{\sigma^2}} \phi_0(y) \right] dy, \quad x \in I.$$

In terms of the operator  $\mathcal{F}_{00}$ , the above equality reads

$$R_0 e^{\frac{(c-\mu)^2}{2\sigma^2}} e^{\frac{(c-\mu)x}{\sigma^2}} \phi_0(x) = \mathcal{F}_{00} \left[ e^{\frac{(c-\mu)\cdot}{\sigma^2}} \phi_0 \right] (x), \quad x \in I. \quad (2.18)$$

Note that the function  $x \mapsto e^{\frac{(c-\mu)x}{\sigma^2}} \phi_0(x)$  belongs to  $C_{++}(I)$ . Since clearly  $\mathcal{F}_{00}$  is strongly positive and compact, we apply the Kreĭn-Rutman theorem to conclude that  $R_0 e^{\frac{(c-\mu)^2}{2\sigma^2}} = r(\mathcal{F}_{00})$ , which leads to the result.

Consider the equation (1.2) with  $K$  being a Gaussian probability density function as in (2.12). In the case  $\mu = 0$ , this equation is more or less a time-discrete version of the reaction-diffusion equation (1.1). In this case, either extinction occurs for all shifting speed, or there is a critical shifting speed separating extinction and persistence.

In the case  $\mu \neq 0$ , the equation can be used to study the extinction or persistence of a stream-dwelling species under climate change. Theorem 2.8 (3) says that if the stream drives the species to disperse to the left, then the species can only survive when the climate envelope shifts to the right with a relatively slow speed. If the stream drives the species to disperse to the right as in Theorem 2.8 (4), then the species dies out when the climate envelope shifts too slow or too fast to the right. In the former case, the species misses the climate envelope, while in the latter case, the species can not keep up with the shifting climate envelope.

## 2.5 Persistence numerical simulations

In this subsection, we consider some numerical simulations of a simple example to complement the analytical results proven earlier for the persistence criterion. To do so, we first decide on the functional forms for the dispersal kernel, the growth function, and the climate envelope function that satisfy the hypotheses laid out in **(H)** in Section 1. For the dispersal kernel,  $K$ , we consider the Gaussian dispersal kernel

$$K_g(x) = \frac{1}{\sqrt{2\pi\sigma^2}} e^{-\frac{(x-\mu)^2}{2\sigma^2}}, \quad x \in \mathbb{R},$$

where  $\mu$  represents the mean dispersal distance and  $\sigma^2$  is the variance in the dispersal distance. Here we use the subscript  $g$  to stand for Gaussian so as to distinguish it from other dispersal kernels used later. For the growth function,  $f$ , we use the Beverton-Holt function,

$$f(u) = \frac{Ru}{1 + \frac{(R-1)}{K_*}u}, \quad u \geq 0,$$

where  $R$  is the growth rate and  $K_*$  is the carrying capacity. The climate envelope,  $g$ , is assumed to be an indicator function on  $[-\frac{L}{2}, \frac{L}{2}]$ . That is,

$$g(x) = 1_{[-\frac{L}{2}, \frac{L}{2}]}(x), \quad x \in \mathbb{R}.$$

Since  $g$  is identically one in the interval  $[-\frac{L}{2}, \frac{L}{2}]$  and zero elsewhere this means that the suitable habitat for the population is simply the interval  $[-\frac{L}{2}, \frac{L}{2}]$ . Then, the IDE provided in (1.2) with a Gaussian dispersal kernel, an indicator climate envelope function, and a Beverton-Holt growth function becomes

$$u_{n+1}(x) = \int_{-\frac{L}{2}+cn}^{\frac{L}{2}+cn} \frac{1}{\sqrt{2\pi\sigma^2}} e^{-\frac{(x-y-\mu)^2}{2\sigma^2}} \frac{Ru_n(y)}{1 + \frac{(R-1)}{K_*}u_n(y)} dy, \quad x \in \mathbb{R}. \quad (2.19)$$

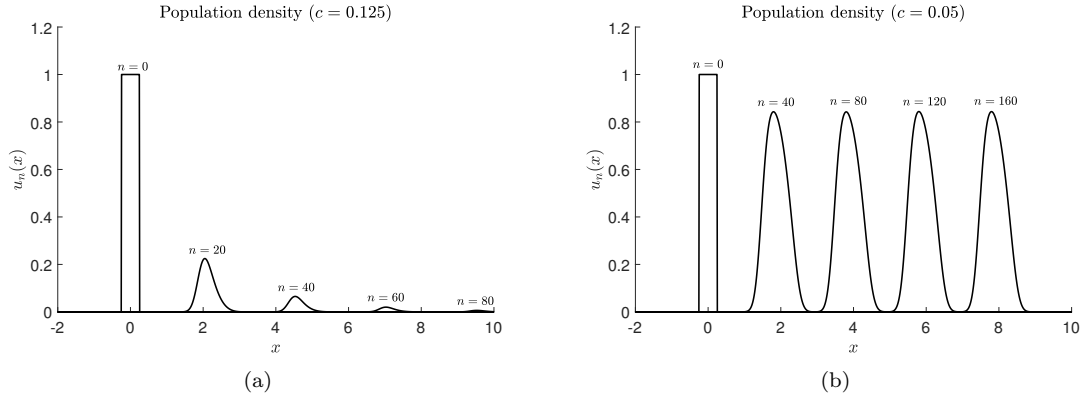


**Fig. 1** A numerical simulation for (2.19). In the two simulations we use the following parameter values:  $R = 1.5$ ,  $K_* = 1$ ,  $\mu = 0$ ,  $\sigma^2 = 0.02$ , and  $L = 1$ . We vary the speed of the shifting habitat from (a)  $c = 0.125$ , to (b)  $c = 0.05$ .

All numerical simulations were performed using the fast Fourier transform technique [26]. This method speeds up the process of quadrature from  $O(n^2)$  to  $O(n \log(n))$  where  $n$  is the number of spatial mesh points. This is done by using the convolution theorem after applying the Fourier transform. The numerical simulations in Figure 1 provide two examples of typical behaviour for (2.19). Figure 1(b) shows that for small values of  $c$ , the population persists and approaches a travelling wave. Figure 1(a) shows that when  $c$  becomes too large, then the population is not able to keep pace with the shifting climate envelope and the population becomes extinct. These simulations depict the persistence theorem provided in Theorem 2.4. There is similar behaviour for the size of the shifting climate envelope. That is, if the length of the shifting climate envelope is too small then the population cannot persist. We provide a plot showing the region of persistence dependent on the speed ( $c$ ) and length ( $L$ ) of the climate envelope. To do this, we numerically approximate the dominant eigenvalue of

$$\lambda\phi(x) = r_0 \int_I K(x-y+c)g(y)\phi(y) dy, \quad x \in I. \quad (2.20)$$

If we again assume the same habitat shifting function as done in the previous example, then (2.20) becomes

$$\lambda\phi(x) = r_0 \int_{-\frac{L}{2}}^{\frac{L}{2}} K(x-y+c)\phi(y) dy, \quad x \in \left[-\frac{L}{2}, \frac{L}{2}\right]. \quad (2.21)$$

To numerically approximate the spectral radius of (2.21), we use the Nyström method. That is, we approximate the integral using the trapezoid rule. Then, our problem becomes

$$\lambda\phi(x_i) = r_0 \frac{L}{2(N-1)} \sum_{j=1}^{N-1} [K(x_i - y_j + c)\phi(y_j) + K(x_i - y_{j+1} + c)\phi(y_{j+1})]. \quad (2.22)$$

for  $i = 1, \dots, N$ . By letting

$$A_{i1} = r_0 \frac{L}{2(N-1)} K(x_i - y_1 + c), \quad (2.23)$$

$$A_{ij} = r_0 \frac{L}{N-1} K(x_i - y_j + c), \text{ for } 2 \leq j \leq N-1, \text{ and} \quad (2.24)$$

$$A_{iN} = r_0 \frac{L}{2(N-1)} K(x_i - y_N + c), \quad (2.25)$$

we obtain the following linear system

$$\lambda\phi = A\phi, \quad (2.26)$$

where  $A = (A_{ij})_{1 \leq i, j \leq N}$ . From this point, we can now calculate the spectral radius by using standard matrix techniques since we have reduced the problem from infinite to finite-dimensional.

For comparison in our simulations we also consider a Laplace dispersal kernel

$$K_l(x) = \frac{1}{2b} e^{-|x-\mu|/b}, \quad x \in \mathbb{R},$$

where  $\mu$  is the mean and  $2b^2$  is the variance. Here, the subscript  $l$  stands for Laplace.

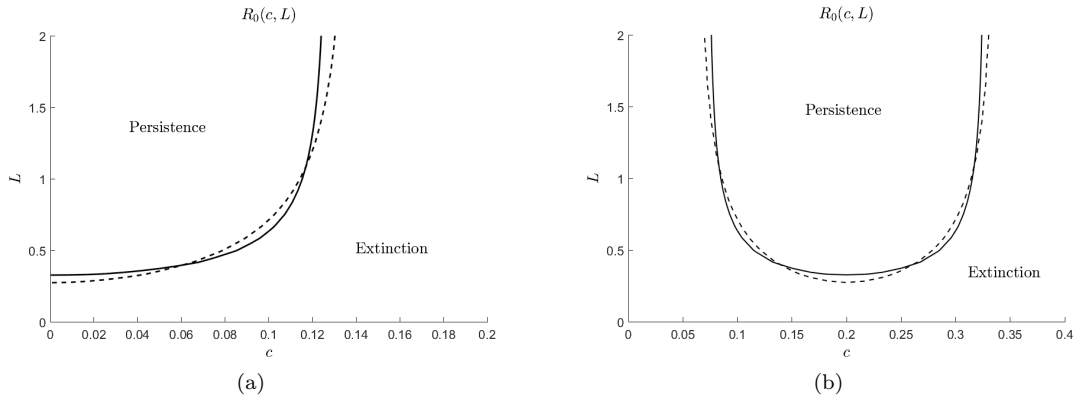


**Fig. 2** A contour plot for the spectral radius of (2.21). The solid and dashed curves are the level sets for  $R_0(c, L) = 1$  for the Gaussian and Laplace dispersal kernels respectively. In these simulations we use the following parameter values,  $r_0 = 1.5$ ,  $\sigma^2 = 0.02$ ,  $b = 0.1$  and (a)  $\mu = 0$  (b)  $\mu = 0.2$ . These parameters were chosen so that both dispersal kernels have the same mean and variance.

In Figure 2, we find the dominant eigenvalue of (2.26) by varying the size and the shifting speed of the climate envelope. The solid (resp. dashed) curve is the level set for  $R_0(c, L) = 1$  with a Gaussian (resp. Laplace) dispersal kernel. From Figure 2(a) and 2(b), if we fix  $c$ , we can see that there is a minimum length of the climate envelope to obtain persistence. This agrees with the result proven in Theorem 2.6. there exists a critical value of  $L$ ,  $L_* > 0$ , such that  $R_0(L) \leq 1$  for  $L \in (0, L_*]$  and  $R_0(L) > 1$  for  $L > L_*$ . This critical value,  $L_*$ , is called the critical domain size. By fixing  $L$ , Figure 2(a) and 2(b) illustrate the results of Theorem 2.8. In particular, Figure 2(a) shows statement (3) of Theorem 2.8 that there is a critical value of  $c$ ,  $c_*$ , such that  $R_0 > 1$  if  $c \in (0, c_*)$  and  $R_0 \leq 1$  for  $c \geq c_*$ . Figure 2(b) provides a numerical example for statement (4) of Theorem 2.8. That is, there exist  $0 \leq c_*^1 < c_*^2 < \infty$  such that  $R_0 > 1$  for  $c \in (c_*^1, c_*^2)$  and  $R_0 \leq 1$  for  $c \in (0, c_*^1] \cup [c_*^2, \infty)$ . The plots in Figure 2 also suggest that the results proven in Theorem 2.8 should also hold for the Laplace kernel.

### 3 Inside dynamics

We study the inside dynamics of (1.2) when  $R_0 > 1$ . Let us consider an arbitrary solution  $\{u_n^*\}_n$  of (1.2) with initial condition  $u_0^* \in C_+(\mathbb{R})$  being non-zero on  $I$ . By Theorem 2.4(2),  $u_n^*(x) \rightarrow w^*(x - cn)$  uniformly in  $x \in \mathbb{R}$  as  $n \rightarrow \infty$ , where  $\{w^*(\cdot - cn)\}_{n \in \mathbb{Z}}$  is the unique travelling wave of (1.2) given in Theorem 2.4(1).

To study the inside dynamics of  $\{u_n^*\}_n$ , we separate it into different neutral fractions as follows: let

$$u_0^* = \sum_{i=1}^N v_0^i,$$

where  $N \geq 1$  and  $v_0^i \in C_+(\mathbb{R}) \setminus \{0\}$  for each  $i = 1, \dots, N$ . For each  $i = 1, \dots, N$ , let us consider the solution  $\{v_n^i\}_n$  of

$$v_{n+1}^i(x) = \int_{\mathbb{R}} K(x - y)g(y - cn)h(u_n^*(y))v_n^i(y)dy, \quad x \in \mathbb{R},$$

with initial condition  $v_0^i$ , where

$$h(u) = \begin{cases} f'(0), & u = 0, \\ \frac{f(u)}{u}, & u > 0. \end{cases}$$

By the uniqueness of solutions, it is easy to see that  $u_n^* = \sum_{i=1}^N v_n^i$  for all  $n \in \mathbb{N}_0$ .

We are interested in asymptotic behaviours of  $v_n^i$  as  $n \rightarrow \infty$  for each  $i$ . Here, we consider two cases about the solution  $\{u_n^*\}_n$  or the initial condition  $u_0^*$ .

- Special case:  $u_0^* = w^*$  so that  $u_n^* = w^*(\cdot - cn)$  for  $n \in \mathbb{N}_0$ ;
- General case: a general initial condition  $u_0^* \in C_+(\mathbb{R})$  being non-zero on  $I$ .

These two cases are investigated in Subsection 3.1 and Subsection 3.2, respectively. In Subsection 3.3, we provide numerical evidence.

### 3.1 Inside dynamics of the travelling wave

We first investigate the case of  $u_n^* = w^*(\cdot - cn)$  for  $n \in \mathbb{N}_0$ . We prove the following theorem.

**Theorem 3.1** *Suppose  $R_0 > 1$ . Let  $v_0 \in C_+(\mathbb{R})$  be a portion of  $w^*$ , that is,  $0 \not\equiv v_0 \leq w^*$ . Consider the solution  $\{v_n\}_n$  of*

$$v_{n+1}(x) = \int_{\mathbb{R}} K(x-y)g(y-cn)h(w^*(y-cn))v_n(y)dy, \quad x \in \mathbb{R} \quad (3.1)$$

with initial condition  $v_0$ . Then there exists a constant  $p := p(v_0) \in [0, 1]$  such that

$$v_n(x+cn) \rightarrow pw^*(x) \quad \text{uniformly in } x \in \mathbb{R} \text{ as } n \rightarrow \infty.$$

Moreover, if, in addition,  $v_0 \not\equiv 0$  on  $I$ , then  $p > 0$ .

We remark that the constant  $p = p(v_0)$  in the statement of Theorem 3.1 can be determined in an implicit way (see (3.5) below).

*Proof (Proof of Theorem 3.1)* We assume  $v_0 \not\equiv 0$  on  $I$ , otherwise  $v_n \equiv 0$  for all  $n \geq 1$ . In the moving frame, (3.1) can be written as

$$v_{n+1}(x+c(n+1)) = \int_{\mathbb{R}} K(x-y+c)g(y)h(w^*(y))v_n(y+cn)dy, \quad x \in \mathbb{R}.$$

Therefore,  $w_n := v_n(\cdot + cn)$  satisfies

$$w_{n+1}(x) = \int_{\mathbb{R}} K(x-y+c)g(y)h(w^*(y))w_n(y)dy, \quad x \in \mathbb{R}.$$

In particular,

$$w_{n+1}(x) = \int_I K(x-y+c)g(y)h(w^*(y))w_n(y)dy, \quad x \in I.$$

Clearly, to finish the proof, it is equivalent to prove

$$w_n \rightarrow pw^* \quad \text{in } C(I) \text{ as } n \rightarrow \infty. \quad (3.2)$$

From now on, we consider  $w_0 = v_0$ ,  $w_n$  and  $w^*$  as functions defined on  $I$ .

For convenience, let us define the map  $\mathcal{G} : C(I) \rightarrow C(I)$  by setting

$$\mathcal{G}[u](x) = \int_I K(x-y+c)g(y)h(w^*(y))u(y)dy, \quad x \in I, \quad (3.3)$$

Using  $\mathcal{G}$ , (3.2) can be restated as

$$\mathcal{G}^n[w_0] \rightarrow pw^* \quad \text{in } C(I) \text{ as } n \rightarrow \infty. \quad (3.4)$$

It remains to prove (3.4). It is easy to check that  $\mathcal{G}$  is strongly positive and compact. Therefore, we can apply Kreĭn-Rutman theorem to  $\mathcal{G}$ . As  $\mathcal{G}[w^*] = w^*$  and  $w^* \in C_{++}(I)$ , we conclude that  $r(\mathcal{G}) = 1$  is an algebraically simple and isolated eigenvalue, and for any  $\lambda \in \sigma(\mathcal{G})$  with  $\lambda \neq 1$ , there holds  $|\lambda| < 1$ .

Moreover, as the eigenvalues of a compact operator can only accumulate at 0, there exist  $r_0 \in (0, 1)$  such that  $\sigma(\mathcal{G}) \setminus \{1\} \subset B_{r_0}$ , where  $B_{r_0}$  is the open disk in  $\mathbb{C}$  centred at 0 with radius  $r_0$ .

Now, let us consider the Riesz projection  $P : C(I) \rightarrow C(I)$  defined by

$$P[u] = \frac{1}{2\pi i} \int_{\gamma} (\xi \mathcal{I}_{C(I)} - \mathcal{G})^{-1} u d\xi, \quad u \in C(I),$$

where  $\gamma$  is the Jordan contour that encloses only 1 from  $\sigma(\mathcal{G})$  and  $\mathcal{I}_{C(I)}$  is the identity operator on  $C(I)$ . It is known that  $P$  is a projection on  $C(I)$ , i.e.,  $P^2 = P$ , with range  $\text{ran}(P) = \{\alpha w^* : \alpha \in \mathbb{R}\}$  the eigenspace associated to 1, which exhausts all fixed points of  $\mathcal{G}$ . Let  $Q = id_{C(I)} - P$ . We know that both  $\text{ran}(P)$  and  $\text{ran}(Q) = \ker(P)$  are invariant subspaces of  $\mathcal{G}$ .

It then follows that

$$\mathcal{G}[w_0] = \mathcal{G}[P[w_0]] + \mathcal{G}[Q[w_0]] = P[w_0] + \mathcal{G}[Q[w_0]],$$

where we used the fact that  $P[w_0]$  is a fixed point of  $\mathcal{G}$ . Applying  $\mathcal{G}$  to the above equality, we find

$$\mathcal{G}^2[w_0] = \mathcal{G}[P[w_0]] + \mathcal{G}^2[Q[w_0]] = P[w_0] + \mathcal{G}^2[Q[w_0]].$$

By iteration, we find

$$\mathcal{G}^n[w_0] = P[w_0] + \mathcal{G}^n[Q[w_0]], \quad n \geq 1.$$

Denote by  $\mathcal{G}_Q$  the part of  $\mathcal{G}$  in  $\text{ran}(Q)$ . Then,  $\mathcal{G}^n[Q[w_0]] = \mathcal{G}_Q^n[Q[w_0]]$  as  $\text{ran}(Q)$  is an invariant subspace of  $\mathcal{G}$ . Since  $\sigma(\mathcal{G}_Q) = \sigma(\mathcal{G}) \setminus \{1\} \subset B_{r_0}$ , we conclude that  $\mathcal{G}^n[Q[w_0]] \rightarrow 0$  in  $C(I)$  as  $n \rightarrow \infty$ , and hence,  $\mathcal{G}^n[w_0] \rightarrow P[w_0]$  in  $C(I)$  as  $n \rightarrow \infty$ , which leads to (3.4) with

$$p = \frac{P[w_0]}{w^*} = \frac{P[v_0]}{w^*}. \tag{3.5}$$

Note that  $P$  is the projection onto the one-dimensional space spanned by  $w^*$ . As a result,  $P[v_0]$  is simply the function  $w^*$  multiplied by some positive constant, and hence,  $p$  is a positive constant. This completes the proof.

Next, we calculate the constant  $p(v_0)$  in the statement of Theorem 3.1 in the case of  $K$  being a Gaussian probability density function as in (2.12).

**Theorem 3.2** *Let the assumptions in Theorem 3.1 be satisfied. In addition, let  $K$  be the Gaussian function given in (2.12). Then,*

$$p(v_0) = \frac{\int_I v_0(x)g(x)f(w^*(x))e^{\frac{2(c-\mu)x}{\sigma^2}} dx}{\int_I w^*(x)g(x)f(w^*(x))e^{\frac{2(c-\mu)x}{\sigma^2}} dx}.$$

*Proof* Recall that the operator  $\mathcal{G}$  is defined in (3.3) and  $K_0$  is defined in (2.13). We calculate

$$\begin{aligned}
\mathcal{G}[u](x) &= \int_I \frac{1}{\sqrt{2\pi\sigma}} e^{-\frac{(x-y+c-\mu)^2}{2\sigma^2}} g(y) h(w^*(y)) u(y) dy \\
&= \int_I \frac{1}{\sqrt{2\pi\sigma}} e^{-\frac{(x-y)^2 + 2(c-\mu)(x-y) + (c-\mu)^2}{2\sigma^2}} g(y) h(w^*(y)) u(y) dy \\
&= e^{-\frac{(c-\mu)x}{\sigma^2}} e^{-\frac{(c-\mu)^2}{2\sigma^2}} \int_I \frac{1}{\sqrt{2\pi\sigma}} e^{-\frac{(x-y)^2}{2\sigma^2}} e^{\frac{(c-\mu)y}{\sigma^2}} g(y) h(w^*(y)) u(y) dy \\
&= e^{-\frac{(c-\mu)x}{\sigma^2}} \int_I K_0(x-y) e^{-\frac{(c-\mu)^2}{2\sigma^2}} g(y) h(w^*(y)) e^{\frac{(c-\mu)y}{\sigma^2}} u(y) dy \\
&= e^{-\frac{(c-\mu)x}{\sigma^2}} \int_I K_0(x-y) \rho(y) e^{\frac{(c-\mu)y}{\sigma^2}} u(y) dy, \quad x \in I,
\end{aligned}$$

where  $\rho(x) = e^{-\frac{(c-\mu)^2}{2\sigma^2}} g(x) h(w^*(x))$  for  $x \in I$ . Multiplying the above equalities by  $\sqrt{\rho}$  yields

$$\sqrt{\rho(x)} e^{\frac{(c-\mu)x}{\sigma^2}} \mathcal{G}[u](x) = \int_I \sqrt{\rho(x)} K_0(x-y) \sqrt{\rho(y)} \left[ \sqrt{\rho(y)} e^{\frac{(c-\mu)y}{\sigma^2}} u(y) \right] dy, \quad x \in I.$$

Defining the operator  $\tilde{\mathcal{G}}$ :

$$\tilde{\mathcal{G}}[u](x) = \int_I \sqrt{\rho(x)} K_0(x-y) \sqrt{\rho(y)} u(y) dy, \quad x \in I,$$

and the multiplication operator  $\mathcal{M}$ :

$$\mathcal{M}[u](x) = \sqrt{\rho(x)} e^{\frac{(c-\mu)x}{\sigma^2}} u(x), \quad x \in I,$$

we find

$$\mathcal{M}\mathcal{G} = \tilde{\mathcal{G}}\mathcal{M}. \quad (3.6)$$

As opposed to the original operator  $\mathcal{G}$ , the operator  $\tilde{\mathcal{G}}$  is symmetric if we consider it as an operator on  $L^2(I)$ . Since

$$\int_I \int_I \sqrt{\rho(x)} K_0(x-y) \sqrt{\rho(y)} dx dy < \infty,$$

the operator  $\tilde{\mathcal{G}}$  is a Hilbert-Schmidt operator, in particular, it is a compact operator. Moreover, the eigenspaces of  $\tilde{\mathcal{G}}$  span  $L^2(I)$ . Recall 1 is an algebraically simple and isolated eigenvalue of  $\mathcal{G}$  and its eigenspace is spanned by  $w^*$ , which is considered as a function on  $I$ . By (3.6), we see that 1 is also an eigenvalue of  $\tilde{\mathcal{G}}$  with  $\mathcal{M}[w^*]$  as an eigenfunction. Since  $\mathcal{M}[w^*] \in C_{++}(I)$  and the kernel  $(x, y) \mapsto \int_I \sqrt{\rho(x)} K_0(x-y) \sqrt{\rho(y)}$  is positive a.e. on  $I \times I$ , we can apply an infinite-dimensional version of the Perron-Frobenius theorem (see [27, 21] or [10, Proposition 4.4]) that 1 is an algebraically simple and isolated eigenvalue of  $\tilde{\mathcal{G}}$ . Therefore, the eigenspace of  $\tilde{\mathcal{G}}$  associated to 1 is spanned by  $\mathcal{M}[w^*]$ . Moreover, there is  $\tilde{r}_0 \in (0, 1)$  such that  $\sigma(\tilde{\mathcal{G}}) \setminus \{1\} \subset B_{\tilde{r}_0}$ , where  $B_{\tilde{r}_0}$  is the open disk in  $\mathbb{C}$  centred at 0 with radius  $\tilde{r}_0$ . Let  $\tilde{P}$  be the orthogonal projection of  $L^2(I)$  onto the eigenspace of  $\tilde{\mathcal{G}}$  associated to 1, that is, the one spanned by  $\mathcal{M}[w^*]$ , and let  $\tilde{Q} = \mathcal{I}_{L^2(I)} - \tilde{P}$ , where  $\mathcal{I}_{L^2(I)}$  is the identity operator on  $L^2(I)$ .

By (3.6), we see  $\mathcal{M}\mathcal{G}^2 = \tilde{\mathcal{G}}\mathcal{M}\mathcal{G} = \tilde{\mathcal{G}}^2\mathcal{M}$ , and hence, by iteration,  $\mathcal{M}\mathcal{G}^n = \tilde{\mathcal{G}}^n\mathcal{M}$  for all  $n \in \mathbb{N}$ . It then follows that

$$p(v_0)\mathcal{M}[w^*] = \mathcal{M}[p(v_0)w^*] = \lim_{n \rightarrow \infty} \mathcal{M}[\mathcal{G}^n[v_0]] = \lim_{n \rightarrow \infty} \tilde{\mathcal{G}}^n[\mathcal{M}[v_0]].$$

Since  $\tilde{\mathcal{G}}^n[\mathcal{M}[v_0]] = \tilde{\mathcal{G}}^n[\tilde{P}[\mathcal{M}[v_0]]] + \tilde{\mathcal{G}}^n[\tilde{Q}[\mathcal{M}[v_0]]] \rightarrow \tilde{P}[\mathcal{M}[v_0]]$  as  $n \rightarrow \infty$ , we find

$$p(v_0)\mathcal{M}[w^*] = \tilde{P}[\mathcal{M}[v_0]] = \frac{\langle \mathcal{M}[v_0], \mathcal{M}[w^*] \rangle_{L^2(I)}}{\|\mathcal{M}[w^*]\|_{L^2(I)}^2} \mathcal{M}[w^*],$$

which leads to the result.

### 3.2 Inside dynamics of general solutions

Now, we consider the general case. Recall that  $\{u_n^*\}_n$  is a solution of (1.2) with  $u_0^* \in C_+(\mathbb{R})$  being non-zero on  $I$ . We prove the following result.

**Theorem 3.3** *Suppose  $R_0 > 1$ . Let  $v_0 \in C_+(\mathbb{R})$  be a portion of  $u_0^*$ , that is,  $0 \not\leq v_0 \leq u_0^*$ . Consider the solution  $\{v_n\}_n$  of*

$$v_{n+1}(x) = \int_{\mathbb{R}} K(x-y)g(y-cn)h(u_n^*(y))v_n(y)dy, \quad x \in \mathbb{R}$$

with initial condition  $v_0$ . Then there exists a constant  $p := p(v_0) \in [0, 1]$  such that

$$v_n(x+cn) \rightarrow pw^*(x) \quad \text{uniformly in } x \in \mathbb{R} \text{ as } n \rightarrow \infty.$$

Moreover, if, in addition,  $v_0 \not\equiv 0$  on  $I$ , then  $p > 0$ .

*Proof* Suppose  $v_0 \not\equiv 0$  on  $I$ , otherwise  $v_n \equiv 0$  for  $n \geq 1$ . Clearly,  $w_n := v_n(\cdot + cn)$  satisfies  $w_0 = v_0$  and

$$\begin{aligned} w_{n+1}(x) &= \int_{\mathbb{R}} K(x-y+c)g(y)h(u_n^*(y+cn))w_n(y)dy \\ &= \int_I K(x-y+c)g(y)h(u_n^*(y+cn))w_n(y)dy, \quad x \in \mathbb{R}. \end{aligned}$$

Note that it is equivalent to consider the equation on  $I$ . Therefore, we consider  $w_n$  and  $u_n^*(\cdot + cn)$  as functions on  $I$  from now on, and hence,

$$w_{n+1}(x) = \int_I K(x-y+c)g(y)h(u_n^*(y+cn))w_n(y)dy, \quad x \in I.$$

As obviously  $\{u_n^*(\cdot + cn)\}_n$  satisfies

$$u_{n+1}^*(x+c(n+1)) = \int_I K(x-y+c)g(y)h(u_n^*(y+cn))u_n^*(y+cn)dy, \quad x \in I,$$

the multiplication of the above equality by constants implies that for each  $\alpha \in \mathbb{R}$ ,

$$w_n^\alpha := \alpha u_n^*(\cdot + cn), \quad n \in \mathbb{N}_0$$

satisfies

$$w_{n+1}^\alpha(x) = \int_I K(x-y+c)g(y)h(u_n^*(y+cn))w_n^\alpha(y)dy, \quad x \in I.$$

Now, we are ready to start an iterative procedure. Note that  $\min_{x \in I} w_n(x) > 0$  and  $\min_{x \in I} w_n^\alpha > 0$  for all  $n \geq 1$  and  $\alpha > 0$ . For convenience, let us also define the map  $\mathcal{G}_n : C_+(I) \rightarrow C_+(I)$  by setting

$$\mathcal{G}_n[u](x) = \int_I K(x-y+c)g(y)h(u_n^*(y+cn))u(y)dy, \quad x \in I$$

for  $n \geq 1$ . Then,

$$w_{n+1} = \mathcal{G}_n[w_n] \quad \text{and} \quad w_{n+1}^\alpha = \mathcal{G}_n[w_n^\alpha].$$

Let  $\alpha_1 > 0$  be the largest number and  $\beta_1 > 0$  be the smallest number such that

$$\begin{cases} w_1^{\alpha_1} \leq w_1 \leq w_1^{\beta_1} \text{ on } I, \\ \exists x_1, y_1 \in I \text{ s.t. } w_1^{\alpha_1}(x_1) = w_1(x_1) \text{ and } w_1(y_1) = w_1^{\beta_1}(y_1). \end{cases}$$

Assuming none of the above two inequalities is actually an equality (otherwise, we are done) and applying  $\mathcal{G}_1$  to obtain

$$w_2^{\alpha_1} < w_2 < w_2^{\beta_1} \quad \text{on } I,$$

where we used the strong positivity of  $\mathcal{G}_1$ . Then, let  $\alpha_2 > \alpha_1$  be the largest number and  $\beta_2 < \beta_1$  be the smallest number such that

$$\begin{cases} w_2^{\alpha_2} \leq w_2 \leq w_2^{\beta_2} \text{ on } I, \\ \exists x_2, y_2 \in I \text{ s.t. } w_2^{\alpha_2}(x_2) = w_2(x_2) \text{ and } w_2(y_2) = w_2^{\beta_2}(y_2). \end{cases}$$

Assuming none of the above two inequalities is actually an equality (otherwise, we are done) and applying  $\mathcal{G}_2$  to obtain

$$w_3^{\alpha_2} < w_3 < w_3^{\beta_2} \quad \text{on } I.$$

Then, let  $\alpha_3 > \alpha_2$  be the largest number and  $\beta_3 < \beta_2$  be the smallest number such that

$$\begin{cases} w_3^{\alpha_3} \leq w_3 \leq w_3^{\beta_3} \text{ on } I, \\ \exists x_3, y_3 \in I \text{ s.t. } w_3^{\alpha_3}(x_3) = w_3(x_3) \text{ and } w_3(y_3) = w_3^{\beta_3}(y_3). \end{cases}$$

Clearly, we can repeat the above process to obtain the following:

- an increasing sequence  $\{\alpha_n\}_n \subset (0, \infty)$  and a decreasing sequence  $\{\beta_n\}_n \subset (0, \infty)$ ;
- for each  $n$ , there holds

$$w_n^{\alpha_n} \leq w_n \leq w_n^{\beta_n} \quad \text{on } I \tag{3.7}$$

with the assumption that none of the above two inequalities is actually an equality (otherwise we are done);

– for each  $n$ , there are  $x_n, y_n \in I$  such that

$$w_n^{\alpha_n}(x_n) = w_n(x_n) \quad \text{and} \quad w_n(y_n) = w_n^{\beta_n}(y_n). \quad (3.8)$$

Set

$$\alpha_\infty = \lim_{n \rightarrow \infty} \alpha_n \quad \text{and} \quad \beta_\infty = \lim_{n \rightarrow \infty} \beta_n.$$

Trivially,  $\alpha_\infty \leq \beta_\infty$ . If  $\alpha_\infty = \beta_\infty$ , we find

$$\|w_n^{\alpha_n} - w_n^{\beta_n}\|_{C(I)} \leq |\alpha_n - \beta_n| \|u^*(\cdot + cn)\|_{C(I)} \rightarrow 0 \quad \text{as} \quad n \rightarrow \infty,$$

where the boundedness of  $\{\|u_n^*(\cdot + cn)\|_{C(I)}\}_n$  follows from the fact that  $u_n^*(\cdot + cn) \rightarrow u^*$  in  $C(I)$  as  $n \rightarrow \infty$ . The result of the theorem then follows readily from (3.7). Therefore, it remains to show that  $\alpha_\infty = \beta_\infty$ .

For contradiction, let us assume  $\alpha_\infty < \beta_\infty$ . We are going to find some  $n_0 \gg 1$  and some  $0 < \delta_0 \ll 1$  such that

$$w_{n_0} + \delta_0 \leq \beta_\infty w^* \quad \text{and} \quad \|w_{n_0}^{\beta_{n_0}} - \beta_\infty w^*\|_{C(I)} \leq \frac{\delta_0}{2}, \quad (3.9)$$

which says particularly that  $w_{n_0}$  and  $w_{n_0}^{\beta_{n_0}}$  can not touch, and therefore, contradicts the second equality in (3.8).

To do so, we write for each  $n$

$$w_n = w_n \mathbf{1}_{[w_n > \beta_\infty w^*]} + w_n \mathbf{1}_{[w_n \leq \beta_\infty w^*]}.$$

Applying  $\mathcal{G}_n$  to the above equation, we find

$$\begin{aligned} w_{n+1}(x) - \beta_\infty w^*(x) &= \int_{[w_n > \beta_\infty w^*]} K(x-y+c)g(y)h(u_n^*(y+cn))w_n(y)dy \\ &\quad + \int_{[w_n \leq \beta_\infty w^*]} K(x-y+c)g(y)h(u_n^*(y+cn))w_n(y)dy - \beta_\infty w^*(x) \\ &= \int_{[w_n > \beta_\infty w^*]} K(x-y+c)g(y)h(u_n^*(y+cn))w_n(y)dy \\ &\quad + \int_{[w_n \leq \beta_\infty w^*]} K(x-y+c)g(y)h(u_n^*(y+cn))\beta_\infty w^*(y)dy - \beta_\infty w^*(x) \\ &\quad + \int_{[w_n \leq \beta_\infty w^*]} K(x-y+c)g(y)h(u_n^*(y+cn))[w_n(y) - \beta_\infty w^*(y)]dy \\ &= A_{n+1}(x) + B_{n+1}(x), \end{aligned}$$

where

$$\begin{aligned} A_{n+1}(x) &= \int_{[w_n > \beta_\infty w^*]} K(x-y+c)g(y)h(u_n^*(y+cn))w_n(y)dy \\ &\quad + \int_{[w_n \leq \beta_\infty w^*]} K(x-y+c)g(y)h(u_n^*(y+cn))\beta_\infty w^*(y)dy - \beta_\infty w^*(x), \\ B_{n+1}(x) &= \int_{[w_n \leq \beta_\infty w^*]} K(x-y+c)g(y)h(u_n^*(y+cn))[w_n(y) - \beta_\infty w^*(y)]dy. \end{aligned}$$

For  $A_{n+1}$ , we can rewrite it as

$$A_{n+1}(x) = A_{n+1}^1(x) - A_{n+1}^2(x) + A_{n+1}^3(x),$$

where

$$\begin{aligned} A_{n+1}^1(x) &= \int_{[w_n > \beta_\infty w^*]} K(x-y+c)g(y)h(u_n^*(y+cn))w_n(y)dy, \\ A_{n+1}^2(x) &= \int_{[w_n > \beta_\infty w^*]} K(x-y+c)g(y)h(u_n^*(y+cn))\beta_\infty w^*(y)dy, \\ A_{n+1}^3(x) &= \int_I K(x-y+c)g(y)h(u_n^*(y+cn))\beta_\infty w^*(y)dy - \beta_\infty w^*(x). \end{aligned}$$

Since  $w_n \leq w_n^{\beta_n} \rightarrow \beta_\infty w^*$ , the Lebesgue measure of  $[w_n > \beta_\infty w^*]$  converges to 0 as  $n \rightarrow \infty$ . As

$$\sup_n \sup_{x,y \in I} [K(x-y+c)g(y)h(u_n^*(y+cn))w_n(y)] < \infty,$$

we conclude that  $A_{n+1}^1 \rightarrow 0$  in  $C(I)$  as  $n \rightarrow \infty$ . The same reasoning ensures that  $A_{n+1}^2 \rightarrow 0$  in  $C(I)$  as  $n \rightarrow \infty$ . Since  $u_n^*(\cdot + cn) \rightarrow w^*$  in  $C(I)$  as  $n \rightarrow \infty$ , and

$$\int_I K(x-y+c)g(y)h(w^*(y))\beta_\infty w^*(y)dy = \beta_\infty w^*(x), \quad x \in I,$$

we find that  $A_{n+1}^3 \rightarrow 0$  in  $C(I)$  as  $n \rightarrow \infty$ . Hence, there holds

$$A_{n+1} \rightarrow 0 \quad \text{in } C(I) \quad \text{as } n \rightarrow \infty. \quad (3.10)$$

It remains to treat  $B_{n+1}$ . We see that

$$\begin{aligned} |w_n(x) - w_n(z)| &\leq \int_I |K(x-y+c) - K(z-y+c)|g(y)h(u_n^*(y+cn))w_{n-1}(y)dy \\ &\leq C_1 \int_I |K(x-y+c) - K(z-y+c)|dy. \end{aligned}$$

for some  $C_1 > 0$ . That is,  $\{w_n\}_n$  are equi-continuous and have a uniform modulus of continuity. This together with the first equality in (3.8) and the assumption  $\alpha_\infty < \beta_\infty$  ensure the existence of intervals  $I_n \subset I$ ,  $n \gg 1$  satisfying the following conditions:

- $x_n$  is one of the end points of  $I_n$ ;
- $I_n$ ,  $n \gg 1$  are of equal length, namely, there is  $\ell > 0$  such that  $|I_n| = \ell$  for all  $n \gg 1$ ;
- there exists  $\delta > 0$  such that for each  $n \gg 1$ , there holds

$$w_n(x) + \delta \leq \beta_\infty w^*(x), \quad \forall x \in I_n.$$

As  $I_n \subset [w_n \leq \beta_\infty w^*]$ , we deduce

$$\begin{aligned} B_{n+1}(x) &\leq \int_{I_n} K(x-y+c)g(y)h(u_n^*(y+cn))[w_n(y) - \beta_\infty w^*(y)]dy \\ &\leq -\delta \int_{I_n} K(x-y+c)g(y)h(u_n^*(y+cn))dy, \quad x \in I \end{aligned}$$

As  $u_n^*(\cdot + cn) \rightarrow w^*$  in  $C(I)$  as  $n \rightarrow \infty$ , it is easy to see that

$$\delta_1 := \liminf_{n \rightarrow \infty} \inf_{x \in I} \int_{I_n} K(x-y+c)g(y)h(u_n^*(y+cn))dy > 0.$$

Therefore,

$$\max_{x \in I} B_{n+1}(x) \leq -\frac{\delta \delta_1}{2}, \quad n \gg 1. \quad (3.11)$$

Choosing  $\delta_0 = \frac{\delta \delta_1}{3}$ , we conclude from (3.10) and (3.11) that

$$w_{n+1}(x) - \beta_\infty w^*(x) \leq -\delta_0, \quad x \in I$$

for all  $n \gg 1$ . Picking a large enough  $n_0$  gives the first condition in (3.9). The second condition in (3.9) follows readily by choosing  $n_0$  larger if necessary as  $w_n^{\beta_n} \rightarrow \beta_\infty w^*$  in  $C(I)$  as  $n \rightarrow \infty$ .

Hence,  $\alpha_\infty = \beta_\infty$ . It then follows from the construction that  $w_n \rightarrow pw^*$  in  $C(I)$  as  $n \rightarrow \infty$ , where  $p = \alpha_\infty = \beta_\infty$ . Equivalently,  $w_n(x) \rightarrow pw^*(x)$  uniformly in  $x \in \mathbb{R}$  as  $n \rightarrow \infty$ .

The following result follows readily from Theorem 3.3.

**Corollary 3.4** *Suppose  $R_0 > 1$ . Let  $\{u_n^*\}_n$  be an arbitrary solution of (1.2) with  $u_0^* \in C_+(\mathbb{R})$  being non-zero on  $I$ . Let*

$$u_0^* = \sum_{i=1}^N v_0^i,$$

where  $N \geq 1$  and  $v_0^i \in C_+(\mathbb{R})$  for each  $i = 1, \dots, N$ . For each  $i = 1, \dots, N$ , let  $\{v_n^i\}_n$  be the solution of

$$v_{n+1}^i(x) = \int_{\mathbb{R}} K(x-y)g(y-cn)h(u_n^*(y))v_n^i(y)dy, \quad x \in \mathbb{R}$$

with initial condition  $v_0^i$ . Then, for each  $i = 1, \dots, N$ , there exists  $p^i \in [0, 1]$  such that

$$v_n^i(x+cn) \rightarrow p^i w^*(x) \quad \text{uniformly in } x \in \mathbb{R} \text{ as } n \rightarrow \infty.$$

Moreover, there holds  $\sum_{i=1}^N p^i = 1$ .

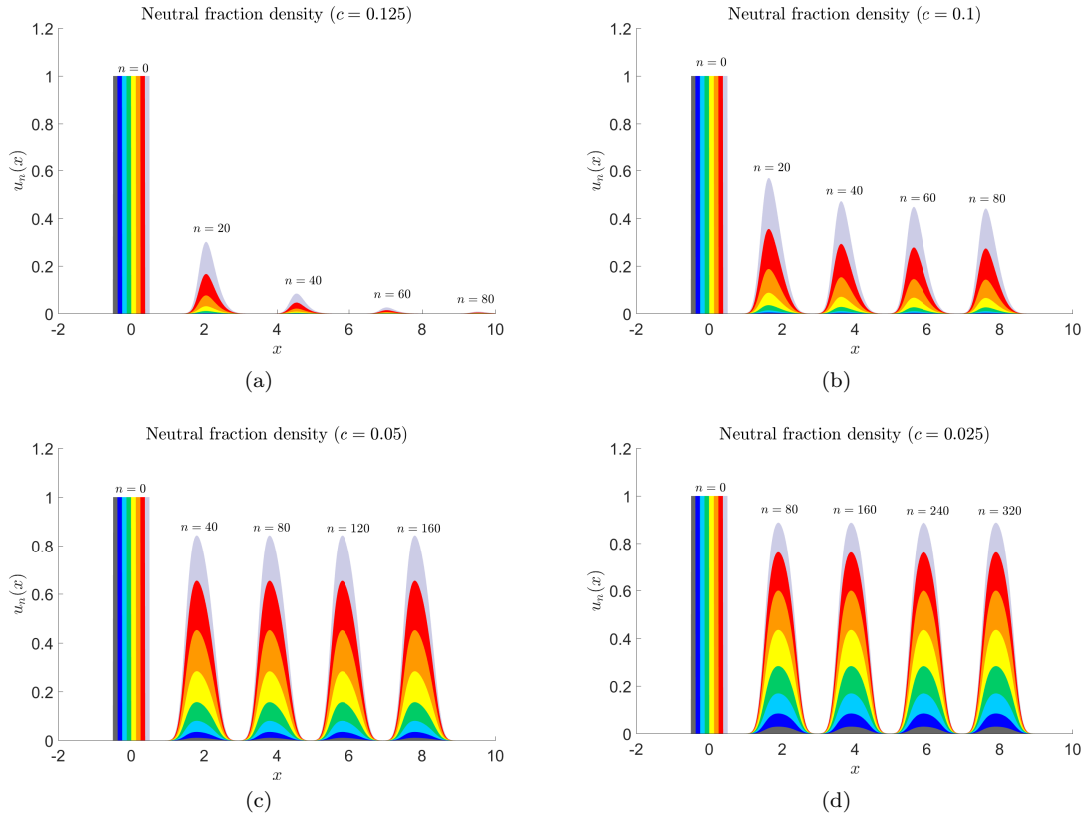


**Fig. 3** A numerical simulation for (2.19). In all four simulations we use the following parameter values:  $R = 1.5$ ,  $K_* = 1$ ,  $\mu = 0$ ,  $\sigma^2 = 0.02$  and  $L = 1$ . We only vary the speed of the shifting habitat from (a)  $c = 0.15$ , (b)  $c = 0.1$ , (c)  $c = 0.05$ , and (d)  $c = 0.025$ .

### 3.3 Inside dynamics numerical simulations

For the inside dynamics simulations, we use a Beverton-Holt growth function, a Gaussian dispersal kernel, and an indicator climate envelope from  $-\frac{L}{2}$  to  $\frac{L}{2}$ . Then, the model that we simulate is given by

$$v_{n+1}^i(x) = \int_{-\frac{L}{2}+cn}^{\frac{L}{2}+cn} \frac{1}{\sqrt{2\pi\sigma^2}} e^{-\frac{(x-y-\mu)^2}{2\sigma^2}} \frac{R}{1 + \frac{(R-1)}{K_*} u_n(y)} v_n^i(y) dy, \quad x \in \mathbb{R}. \quad (3.12)$$

Four different numerical simulations for (3.12) are provided in Figure 3 by altering the speed of the shifting climate envelope. Since the parameter values chosen in Figures 3(a) & 3(c) are the same as those in Figures 1(a) & 1(b) we observe the same overall population level dynamics with the addition that we can track the individual neutral fractions. The initial condition was a top hat distribution, occupying the climate envelope of length  $L$  and comprised of eight disjoint neutral fractions, identical in shape. In particular, we observe the same change of persistence to extinction if  $c$  becomes too large

due to the fact that the spread of solutions cannot keep up with the shifting of the habitat. However, by tracking the neutral fractions, we are able to understand the effect that the shifting habitat speed has on the genetic composition of the population. By comparing Figures 3(b), 3(c), & 3(d) it appears that a decrease in the speed of the shifting habitat causes an increase in the genetic composition of individuals from the rear of the population.

However, when we alter the parameters we can also observe different qualitative behaviour. Figure 4 displays three simulations showing how a decrease in the shifting habitat speed does not always increase genetic heterogeneity.

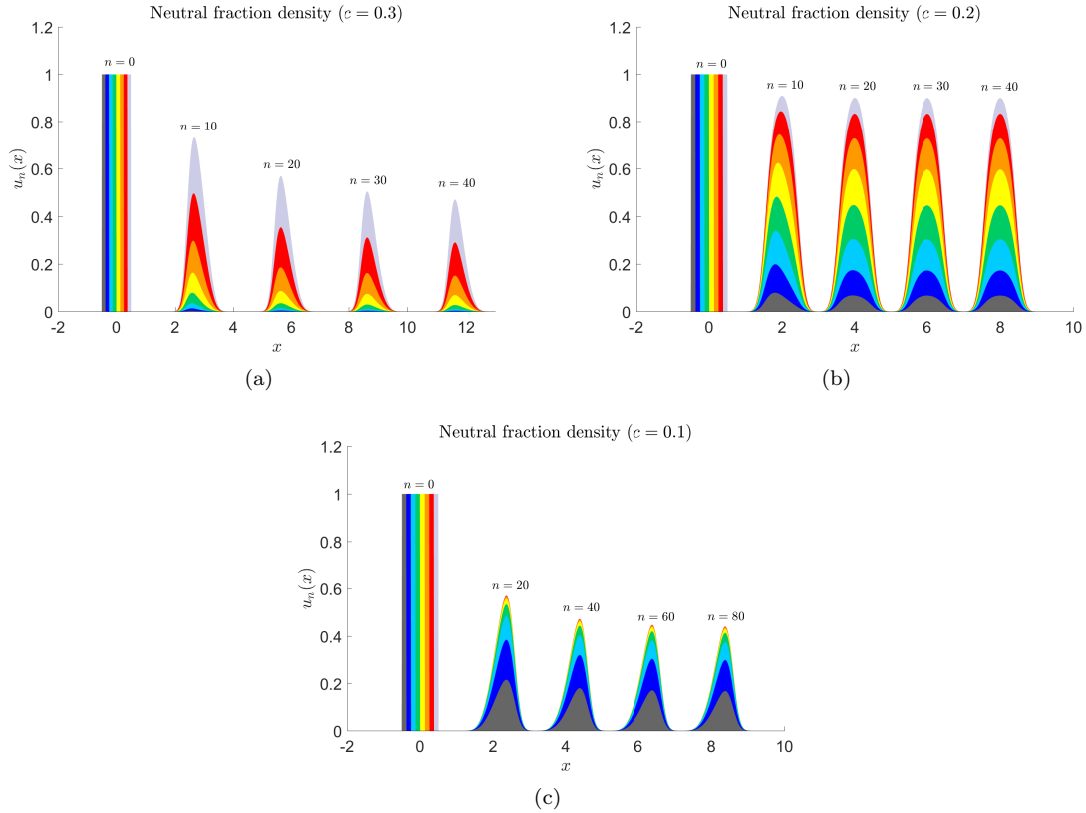


**Fig. 4** A numerical simulation for (2.19). In all three simulations we use the following parameter values:  $R = 1.5$ ,  $K_* = 1$ ,  $\mu = 0.2$ ,  $\sigma^2 = 0.02$  and  $L = 1$ . We only vary the speed of the shifting habitat from (a)  $c = 0.3$ , (b)  $c = 0.2$ , and (c)  $c = 0.1$ .

In Figure 4(a), the speed of the shifting climate envelope is  $c = 0.3$  which is faster than the mean dispersal distance  $\mu = 0.2$ . In this scenario, the neutral fractions at the leading edge have an advantage because it is difficult for the neutral fractions at the rear to keep up with such a fast shifting habitat.

Thus, we can see in Figure 4(a) that the majority of the genetic composition is primarily composed of the three neutral fractions at the leading edge.

In Figure 4(b), the speed of the shifting climate envelope is the mean of the dispersal distance ( $c = \mu = 0.2$ ). The shifting habitat at an intermediate speed increases species evenness. That is, if the climate envelope is not moving too fast or slow relative to the mean dispersal distance of the population, we see a much more even distribution of neutral fractions in the population.

In Figure 4(c), the speed of the shifting climate envelope is  $c = 0.1$  and is half the speed of the mean dispersal distance. Here, we see that neutral fractions at the leading edge are at a disadvantage because they will outspread the suitable climate envelope. This is evident in Figure 4(c), by the genetic composition of the population being dominated by the neutral fractions at the trailing edge of the population.

In order to understand how changing parameters affects the genetic diversity of the population we use a diversity index. A diversity index is a statistic used to measure the diversity of a population. One common diversity index is called the Shannon diversity index [29]. Given that  $p^i(v_0)$  is the asymptotic proportion of individuals in neutral fraction  $i$ , then the index can be computed in the following way

$$H = - \sum_{i=1}^N p^i(v_0) \log(p^i(v_0)) \quad (3.13)$$

where  $N$  is the total number of neutral fractions. Another common diversity index we use is the  $\text{Div}^2$  index [14]. Given that  $p^i(v_0)$  is the asymptotic proportion of individuals in neutral fraction  $i$ , then the index can be computed in the following way

$$\text{Div}^2 = \left( \sum_{i=1}^N (p^i(v_0))^2 \right)^{-1} \quad (3.14)$$

where  $N$  is the total number of neutral fractions. The  $\text{Div}^2$  index is the inverse of the Simpson index, which describes the probability that two individuals sampled randomly at the same time and location belong to the same neutral fraction [28].

To calculate the proportions, we numerically simulate (3.12) using the fast Fourier transform, see Section 2.5 for details. We run the simulations sufficiently long until the solution is at equilibrium. Then, we calculate the proportions at the central spatial location of the suitable domain,  $cn$ , where  $c$  is the speed of the shifting climate envelope and  $n$  is the number of iterations. We perform this for varied values of  $L$  and  $c$  to obtain Figure 5.

Figure 5 provides two plots similar to that of Figure 2 except we now compute the Shannon diversity index for varying parameters  $L$  and  $c$ . This allows us to understand the effect of altering the speed and length of the shifting climate envelope. Initial data were the same as for Figure 3. For a fixed value of  $L$ , we see that in Figure 5(a) the diversity index decreases as  $c$  increases while in Figure 5(b) we see that the diversity index increases and then decreases showing that  $c = \mu = 0.2$  is the optimal value to maximize the Shannon diversity index. It should be noted that this pattern is observed because Shannon diversity index increases as the evenness and richness of the population increases. However, for other diversity indices, the maximum value may not occur when  $c = \mu = 0.2$ .

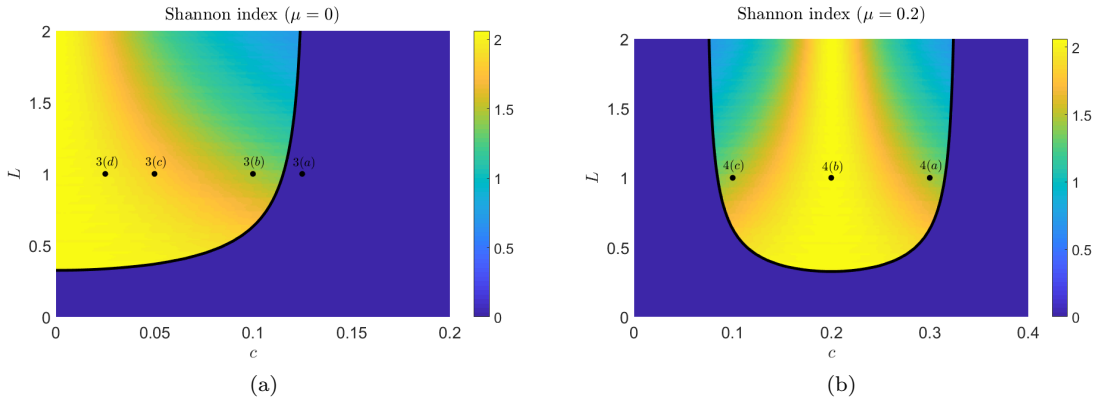


**Fig. 5** A heat map for the Shannon diversity index of (3.12). In these simulations we use the following parameter values,  $R = 1.5$ ,  $K_* = 1$ ,  $\sigma^2 = 0.02$  and (a)  $\mu = 0$  (b)  $\mu = 0.2$ .

To see these differences, a comparison of Figure 5 using other diversity indices is provided in Appendix B.

For completeness, we also calculate the  $\text{Div}^2$  diversity index in Figure 6 by varying  $L$  and  $\sigma^2$  to compare to the previous work [8], where  $c^*$  is the rightward asymptotic spreading speed of the following IDE:

$$u_{n+1}(x) = \int_{\mathbb{R}} \frac{1}{\sqrt{2\pi\sigma^2}} e^{-\frac{(x-y)^2}{2\sigma^2}} \frac{Ru_n(y)}{1 + \frac{(R-1)}{K_*}u_n(y)} dy, \quad x \in \mathbb{R}. \quad (3.15)$$

Moreover, there holds the formula  $c^* = \sqrt{2\sigma^2 \log R}$  (see e.g. [11]). Notice that the pattern here shows that for positive  $c$  and a fixed value of  $L$ , we see that if the population is persistent there is an increase in the diversity index as  $c^*$  increases. This is due to the fact that the dispersal variance,  $\sigma^2$ , is varied while the growth rate,  $R$ , is kept constant for  $c^*$ .

#### 4 Discussion

Section 1 provides some background material and a brief overview of previous deterministic models for climate envelopes. The model we study for the effect of climate change on IDEs was introduced in (1.2). In Section 1, assumptions made on the dispersal kernel, growth function, climate envelope, and shifting speed of the environment are laid out.

Our results begin in Section 2, where we outline the global dynamics of (1.2). Theorem 2.3 outlines the persistence criterion for stationary solutions in terms of the basic reproduction number  $R_0$ . This result is not new, but for completeness, we include the proof in Appendix A. Theorem 2.4, provides the persistence criterion for travelling wave solutions again in terms of the basic reproduction number. A numerical simulation is provided in Figure 1 showing the two dynamics of extinction (Figure 1(a)) and persistence (Figure 1(b)).

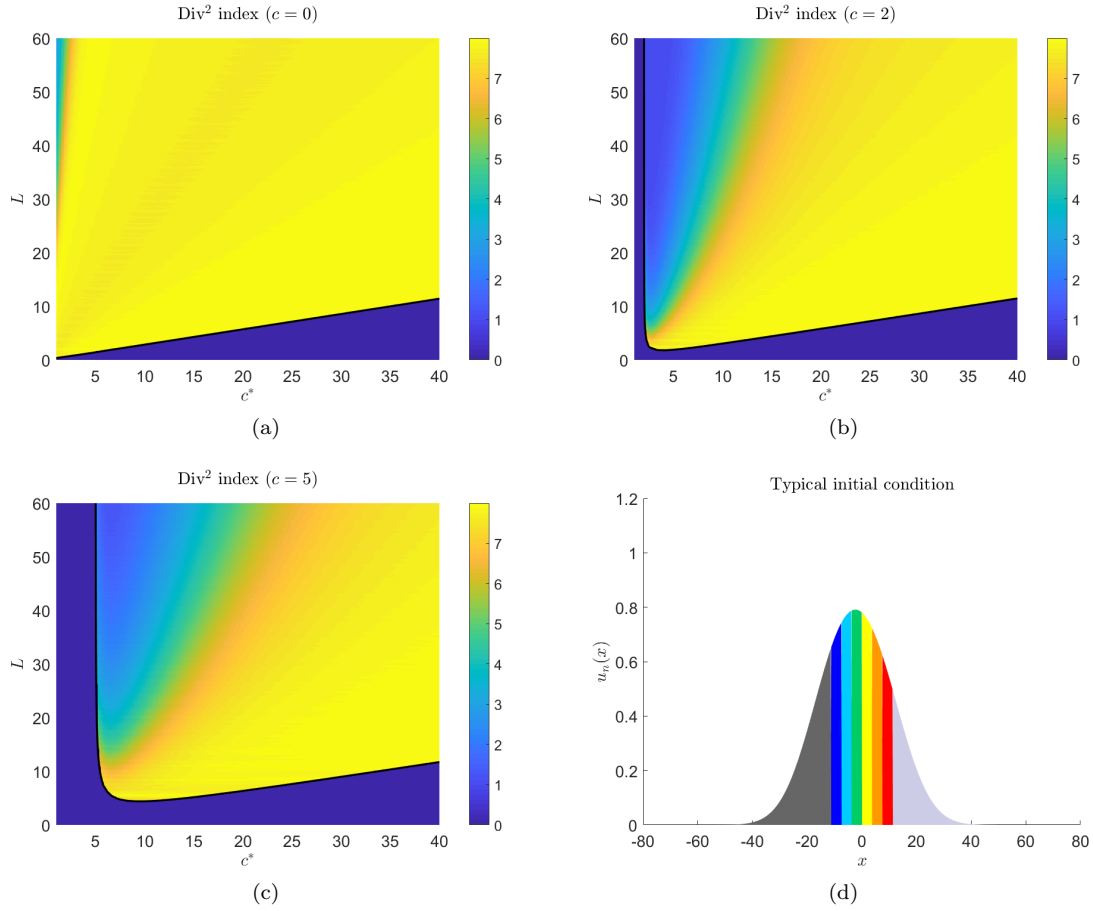


**Fig. 6** A heat map for the  $\text{Div}^2$  diversity index of (3.12). In these simulations we use the following parameter values,  $R = 5$ ,  $K_* = 1$ ,  $\mu = 0$ ,  $\sigma^2 = (c^*)^2/2\log(R)$  and (a)  $c = 0$ , (b)  $c = 2$ , (c)  $c = 5$ . In particular, we keep  $R$  fixed and vary  $\sigma^2$ . A typical initial condition in the form of the traveling wave solution is given in (d) using the parameter values  $R = 5$ ,  $K_* = 1$ ,  $\mu = 0$ ,  $\sigma^2 = 100$ ,  $c = 2$ , and  $L = 30$ .

We go further and analyze the effect that the size of the climate envelope has in the calculation of  $R_0$ . This effect is presented in Theorem 2.6. Here, we assume that the suitable habitat function is an indicator function on the interval  $[-\frac{L}{2}, \frac{L}{2}]$  and show that for persistence there is a critical value  $L_*$  such that  $R_0(L) \leq 1$  for  $L \in (0, L_*]$  and  $R_0(L) > 1$  for  $L > L_*$ . A numerical calculation of  $R_0$  is provided in Figure 2. In Figures 2(a) and 2(b) we see that for a fixed value of  $c$  there is a minimum value of  $L$  required for the population to persist.

We also extend the persistence results by analyzing the effect of the shifting speed of the environment. The result is given in Theorem 2.8. In this theorem, we must assume that the dispersal kernel is Gaussian allowing us to show two interesting results for the persistence of the population

with respect to changing the shifting speed  $c$  of the environment. The first persistence result says that there is a critical speed  $c_*$  such that for  $c \in (0, c_*)$  there is persistence and for  $c \geq c_*$  the population goes extinct. This result holds true for  $\mu \leq 0$  and  $e^{-\frac{\mu^2}{2\sigma^2}} r(\mathcal{F}_{00}) > 1$ . By fixing  $L$  in Figure 2(a), we see this result. The case with  $\mu = 0$  corresponds to the reaction-diffusion equation (1.1), where a unique critical shifting speed separating extinction and persistence is known to exist. However, when  $\mu > 0$ , we see that there exist  $0 \leq c_*^1 < c_*^2 < \infty$  such that  $R_0 > 1$  for  $c \in (c_*^1, c_*^2)$  and  $R_0 \leq 1$  for  $c \in (0, c_*^1] \cup [c_*^2, \infty)$ . That is, there is an intermediate range of speeds that allow for persistence. This is evident in Figure 2(b) by looking at a fixed value of  $L$ . For a stream-dwelling species,  $\mu > 0$  means that the stream drives the species to disperse to the right, and therefore, the species misses the slowly shifting climate envelope and can not catch up with the fast shifting climate envelope.

Moving on from the persistence criterion, the results switch gears into understanding the inside dynamics of (1.2) in Section 3. The first results focus on the inside dynamics of the travelling wave solution. In Theorem 3.1, we show that if the population is persistent, then each neutral fraction converges to a proportion of the travelling wave solution. If we assume that the dispersal kernel is Gaussian, then we can derive an analytic formula for the proportion of each neutral fraction. This formula is given in Theorem 3.2 and is dependent on the initial condition, profile of the travelling wave, shifting speed of the environment, climate envelope function, and dispersal parameters. Next, the result of Theorem 3.1 is extended to general solutions. In Theorem 3.3 we show that if the population is persistent, then each neutral fraction converges to a proportion of the travelling wave solution.

To complement the theoretical results, we provide some numerical simulations for the inside dynamics. Figure 3 is composed of four different simulations by only varying the speed of the shifting climate envelope. In Figure 3(a), the speed of the shifting climate envelope is too fast and we see that the population does not persist. In the Figures 3(b), 3(c), and 3(d), we progressively slow down the speed of the shifting climate envelope. The distribution of the neutral fraction composition changes in each simulation showing that for these parameter values slowing down the speed of the shifting climate envelope increases the evenness of the neutral fraction distribution. In Figure 4, we simply change  $\mu$  to be nonzero and see a different kind of pattern. Again, in Figures 4(a), 4(b), and 4(c), we progressively slow down the speed of the shifting climate envelope. However, at the faster (resp. slower) speeds, the evenness is biased to the leading (resp. rear) neutral fractions, see Figures 4(a) and 4(c). However, in Figure 4(b), the distribution of neutral fractions is very even among all types. This suggests that there is a critical speed of the shifting climate envelope at which the evenness is maximized.

To further explore the assertions from Figures 3 and 4, we employ the use of the Shannon diversity index. The diversity measure is calculated for varying values of the length and the speed of the shifting climate envelope. The heat maps in Figures 5(a) and 5(b) uphold the conjectures drawn from Figures 3 and 4 about the distribution of neutral fractions. For comparison to previous work, we provide more heat maps for the Shannon diversity index in Figure 6 by altering the variance in the dispersal distance of (3.15) and the length of the shifting climate envelope.

The limitations of the model are contingent on the hypotheses made in Section 1. The growth function is assumed to be monotone increasing and does not allow possibility for an Allee effect. As shown in previous work, the Allee effect is known to have a strong influence on the genetic patterns

formed by expansion [7,20]. It is interesting to note that since the climate envelope is compactly supported that the model allows for fat-tailed dispersal kernels.

Our persistence and travelling wave results provide an extension of those in [33]. The neutral genetic diversity results are new to the study of integrodifference equations with a climate envelope. In many ways they are similar to those found by [8] for reaction-diffusion models. However, there are subtle differences. For example the diversity index structure of the wave shown in Figure 6 is different than that shown in Figure 4 of [8]. We believe that this arises due to a fundamental difference in the integrodifference and reaction-diffusion formulations. The integrodifference formulation truncates all populations that disperse outside the climate envelope within a single time step, whereas the reaction-diffusion formulation allows for gradual decline of populations that fall outside the climate envelope. This means that, although the methods for setting up the initial data were identical for the two formulations, the resulting dynamics have different effects on the gene fractions that fall outside the climate envelope: the reaction-diffusion formulation allows them to linger whereas the integrodifference formulation truncates them immediately. This has a concomitant impact on the diversity index, particularly near the lower (small  $L$ ) boundary in Figure 6.

One area for future research is to understand the effects of stochasticity and environmental uncertainty on results of the sort given in this paper. Some initial work in this direction is given in [5], but much remains to be done.

### A Proof of Theorem 2.3

This section is devoted to the proof of Theorem 2.3. We first present some preparatory results.

The following lemma is an immediate consequence of the stationary solution equation.

**Lemma A.1** *Let  $w$  be a stationary solution of (2.2). Then  $w \in C_+(I)$ . If, in addition,  $w \not\equiv 0$ , then  $w \in C_{++}(I)$ .*

The next result gives the nonlinear comparison principle.

**Lemma A.2** *Let  $\bar{w}, \underline{w} \in C_+(I)$  satisfy  $\bar{w} \geq \mathcal{F}[\bar{w}]$  and  $\underline{w} \leq \mathcal{F}[\underline{w}]$ , respectively. If  $\bar{w} \not\equiv 0$ , then  $\bar{w} \geq \underline{w}$ .*

*Proof* Clearly, the conditions on  $\bar{w}$  imply that  $\bar{w} \in C_{++}(I)$ . We assume that  $\underline{w} \not\equiv 0$ , otherwise there is nothing to prove. Define

$$\alpha_* := \inf \{ \alpha > 0 : \alpha \bar{w} \geq \underline{w} \}.$$

By the continuity of  $\bar{w}$  and  $\underline{w}$ ,  $\alpha_* \bar{w} \geq \underline{w}$ . Moreover, there exists  $x_0 \in I$  such that  $\alpha_* \bar{w}(x_0) = \underline{w}(x_0)$ .

We show  $\alpha_* \leq 1$  which leads to the result of the lemma. Suppose  $\alpha_* > 1$  for contradiction. Clearly,

$$0 \geq \int_I K(x_0 - y + c)g(y) [\alpha_* f(\bar{w}(y)) - f(\underline{w}(y))] dy.$$

As there holds

$$\alpha_* f(\bar{w}(y)) = \alpha_* \bar{w}(y) \frac{f(\bar{w}(y))}{\bar{w}(y)} > \alpha_* \bar{w}(y) \frac{f(\alpha_* \bar{w}(y))}{\alpha_* \bar{w}(y)} = f(\alpha_* \bar{w}(y)) > f(\underline{w}(y)), \quad \forall y \in I,$$

where we used **(H)**-(2), we find

$$\int_I K(x_0 - y + c)g(y) [\alpha_* f(\bar{w}(y)) - f(\underline{w}(y))] dy > 0,$$

which leads to a contradiction.

The above lemma leads immediately to the uniqueness of non-zero stationary solution of (2.2).

**Corollary A.3** *There exists at most one non-zero stationary solution of (2.2).*

The following comparison principle for sub- and super-solutions of (2.2) is trivial.

**Lemma A.4** *Let  $\{\bar{w}_n\}_n \subset C_+(I)$  and  $\{\underline{w}_n\}_n \subset C_+(I)$  satisfy  $\bar{w}_{n+1} \geq \mathcal{F}[\bar{w}_n]$  and  $\underline{w}_{n+1} \leq \mathcal{F}[\underline{w}_n]$ , respectively. If  $\bar{w}_0 \geq \underline{w}_0$ , then  $\bar{w}_n \geq \underline{w}_n$  for all  $n$ .*

Now, we are ready to prove Theorem 2.3. We first prove Theorem 2.3(1).

*Proof (Proof of Theorem 2.3(1))* Suppose  $R_0 \leq 1$  first. Clearly, 0 is a stationary solution of (2.2). It remains to show that positive stationary solutions do not exist in this case. For contradiction, let us suppose the existence of a positive stationary solution  $w$  of (2.2). By Lemma A.1,  $\min_I w > 0$ . By (H)-(2),

$$f(w(y)) = w(y) \frac{f(w(y))}{w(y)} < r_0 w(y), \quad y \in I,$$

which implies that  $w(x) < \mathcal{F}_0[w](x)$  for all  $x \in I$ . Therefore, we can find some  $\delta \in (0, 1)$  such that  $w \leq (1 - \delta)\mathcal{F}_0[w]$ . We then iterate to obtain

$$w \leq (1 - \delta)^n \mathcal{F}_0^n[w], \quad \forall n \in \mathbb{N}.$$

Recall that  $\phi_0 \in C_{++}(I)$  is the eigenfunction associated to  $R_0$ . We may assume, without loss of generality, that  $w \leq \phi_0$ . It then follows that  $\mathcal{F}_0^n[w] \leq \mathcal{F}_0^n[\phi_0] = R_0^n \phi_0 \leq \phi_0$ , which leads to

$$w \leq (1 - \delta)^n \phi_0, \quad \forall n \in \mathbb{N}.$$

This yields  $w \equiv 0$ . It is a contradiction.

Now, suppose  $R_0 > 1$ . By Lemma A.1 and Corollary A.3, it suffices to find one positive stationary solution of (2.2). To do so, let us consider for  $\epsilon > 0$  the sequence  $\{w_n^\epsilon\}_n$  defined by

$$w_0^\epsilon = \epsilon \phi_0 \quad \text{and} \quad w_{n+1}^\epsilon = \mathcal{F}[w_n^\epsilon], \quad n \in \mathbb{N}_0.$$

Let  $\delta_0 > 0$  be such that  $\frac{R_0}{1+\delta_0} > 1$ . It is clear that  $R_0 = r(\mathcal{F}_0) \leq \|\mathcal{F}_0\| \leq r_0 = f'(0)$ . Since the limit  $\lim_{\epsilon \rightarrow 0^+} \frac{f(\epsilon \phi_0(x))}{\epsilon \phi_0(x)} = f'(0)$  is uniform in  $x \in I$ , we can find some  $\epsilon_0 > 0$  such that  $\frac{f(\epsilon_0 \phi_0)}{\epsilon_0 \phi_0} \geq \frac{R_0}{1+\delta_0}$ . It then follows the assumption on  $f$  that  $\frac{f(\epsilon \phi_0)}{\epsilon \phi_0} \geq \frac{R_0}{1+\delta_0}$  for all  $\epsilon \in (0, \epsilon_0]$ . We see that

$$w_1^\epsilon = \int_I K(\cdot - y + c)g(y)\epsilon \phi_0 \frac{f(\epsilon \phi_0)}{\epsilon \phi_0} dy \geq \frac{R_0}{1+\delta_0} \mathcal{F}_0[\epsilon \phi_0] = \frac{R_0}{1+\delta_0} \epsilon \phi_0 > \epsilon \phi_0$$

for all  $\epsilon \in (0, \epsilon_0]$ . It then follows from Lemma A.4 that  $w_{n+1}^\epsilon \geq w_n^\epsilon$  for all  $\epsilon \in (0, \epsilon_0]$ .

Let us fix any  $\epsilon \in (0, \epsilon_0]$ . By the boundedness of  $f$ , it is clear that  $\{w_n^\epsilon\}$  is uniformly bounded, and hence, the limit function  $w_* := \lim_{n \rightarrow \infty} w_n^\epsilon$  is well-defined. It is easy to see that  $w_*$  is a positive stationary solution of (2.2). The upper bound on  $w_*$  as in the statement is trivial. This completes the proof.

We denote by  $w_*$  the unique positive stationary solution of (2.2) when  $R_0 > 1$ . In the proof of Theorem 2.3(1), we have proven the following result.

**Corollary A.5** *There exists  $\epsilon_0 > 0$  such that for any  $\epsilon \in (0, \epsilon_0]$ , the sequence  $\{\mathcal{F}^n[\epsilon \phi_0]\}_n$  is increasing and converges in  $C(I)$  to  $w_*$  as  $n \rightarrow \infty$ .*

*Proof* We only need to point out that the convergence in  $C(I)$  comes from Dini's theorem.

Finally, we prove Theorem 2.3(2).

*Proof (Proof of Theorem 2.3(2))* For  $M \geq \sup_{u \in [0, \infty)} f(u)$ , we have  $\mathcal{F}[M] < M$ . It follows that  $\{\mathcal{F}^n[M]\}_n$  is a decreasing sequence. By Theorem 2.3 and Dini's theorem,

$$\mathcal{F}^n[M] \rightarrow \begin{cases} 0, & \text{if } R_0 \leq 1, \\ w_*, & \text{if } R_0 > 1 \end{cases} \quad \text{in } C(I) \text{ as } n \rightarrow \infty.$$

This together with Lemma A.4 yield the result in the case  $R_0 \leq 1$ . In the case of  $R_0 > 1$ , we can find some  $\epsilon_0 > 0$  and  $M_0 > 0$  such that  $\epsilon_0 \phi_0 \leq w_1 \leq M_0$ . We then conclude the result from Lemma A.4 and Corollary A.5.

## B Comparison of Figure 5 with other diversity indices

To make a complete analysis of the patterns seen in Figure 5 we provide similar plots for different diversity measures. We consider the diversity index

$$\text{Div}^q = \left( \sum_{i=1}^N (p^i)^q \right)^{\frac{1}{1-q}}. \quad (\text{B.1})$$

for  $0 < q < 1$  and  $1 < q < \infty$ . In the limit as  $q \rightarrow 1$ , it can be shown that

$$\text{Div}^1 = \exp \left( - \sum_{i=1}^N p^i \ln(p^i) \right), \quad (\text{B.2})$$

yielding that  $\text{Div}^1$  is the exponential of the Shannon diversity index. When  $q = 0$  the diversity index becomes the species richness and when  $q = \infty$  the diversity index becomes a measure of species evenness, given by the maximum  $p^i$  value. In Figures 7 and 8 we provide plots constructed in the same manner as Figure 5.

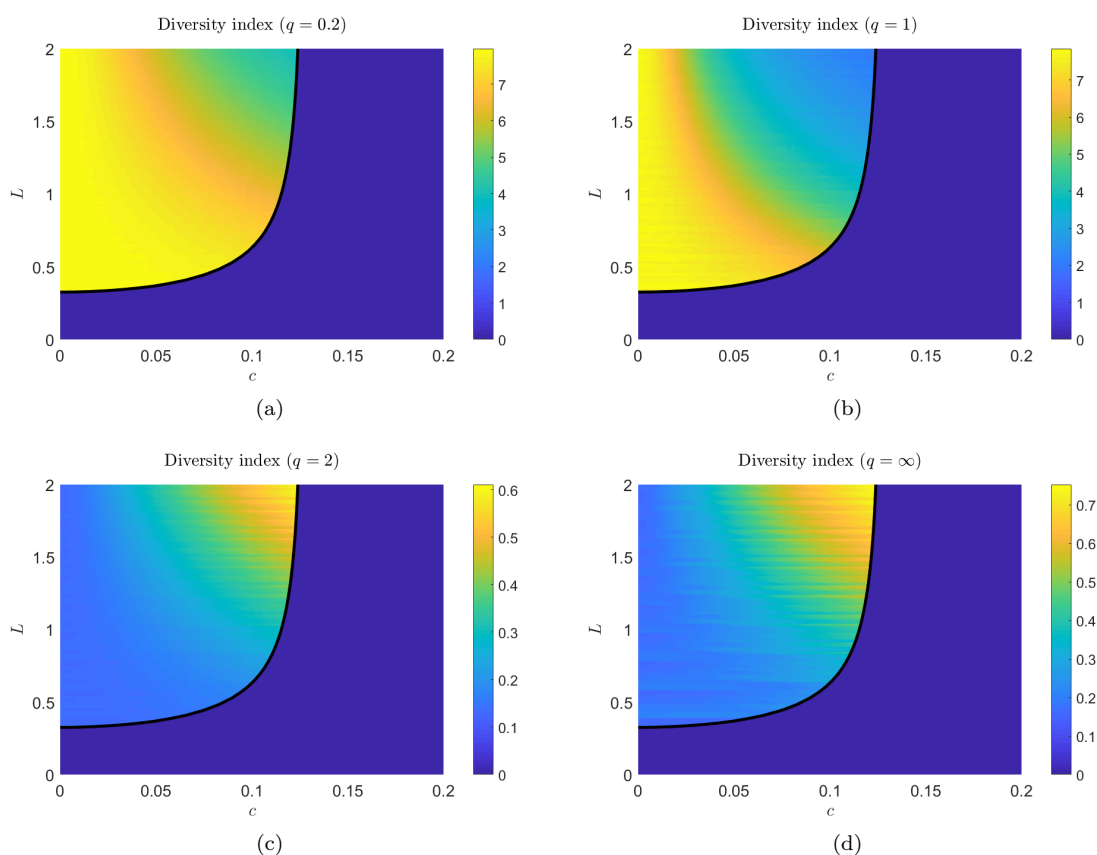


**Fig. 7** A heat map for the  $\text{Div}^q$  diversity index of (3.12) where (a)  $q = 0.2$ , (b)  $q = 1$ , (c)  $q = 2$ , and (d)  $q = \infty$ . In these simulations we use the following parameter values,  $R = 1.5$ ,  $K_* = 1$ ,  $\sigma^2 = 0.02$  and  $\mu = 0$ .

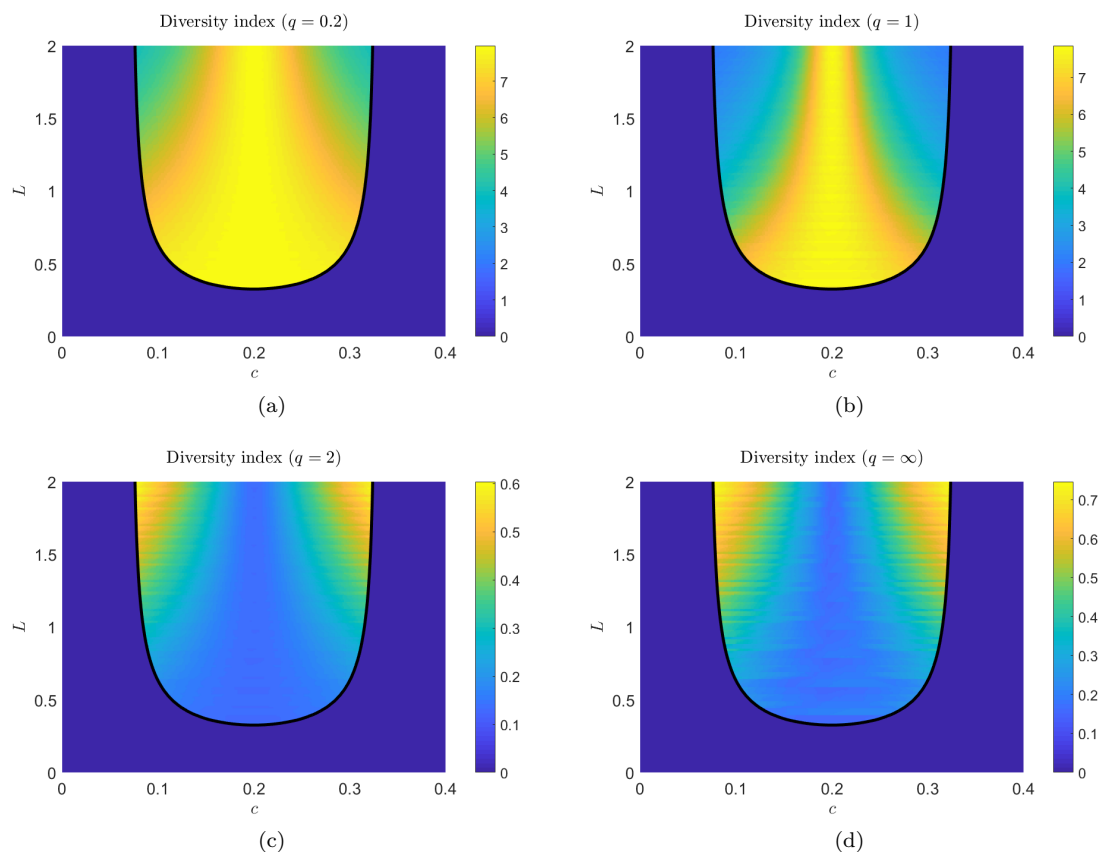


**Fig. 8** A heat map for the  $\text{Div}^q$  diversity index of (3.12) where (a)  $q = 0.2$ , (b)  $q = 1$ , (c)  $q = 2$ , and (d)  $q = \infty$ . In these simulations we use the following parameter values,  $R = 1.5$ ,  $K_* = 1$ ,  $\sigma^2 = 0.02$  and  $\mu = 0.2$ .

## References

1. O. Bonnefon, J. Coville, J. Garnier and L. Roques, Inside dynamics of solutions of integro-differential equations. *Discrete Contin. Dyn. Syst. Ser. B* 19, no. 10, 3057-3085 (2014).
2. M. Bálint, S. Domisch, C. H. M. Engelhardt, P. Haase, S. Lehrian, J. Sauer, K. Theissingner, S. U. Pauls, and C. Nowak, Cryptic biodiversity loss linked to global climate change. *Nature Climate Change* 1(6), 313-318 (2011).
3. H. Berestycki, O. Diekmann, C. J. Nagelkerke and P. A. Zegeling, Can a species keep pace with a shifting climate? *Bull. Math. Biol.* 71, no. 2, 399-429 (2009).
4. R. J. H. Beverton and S. J. Holt, On the dynamics of exploited fish populations. Her Majesty's Stationery Office, London (1957).
5. J. Bouhours and M. A. Lewis, Climate change and integrodifference equations in a stochastic environment. *Bull. Math. Biol.* 78(9), 1866-1903 (2016).
6. M. D. Donsker and S. R. S. Varadhan, On a variational formula for the principal eigenvalue for operators with maximum principle. *Proc. Nat. Acad. Sci. U.S.A.* 72, 780-783 (1975).
7. J. Garnier, T. Giletti, F. Hamel and L. Roques, Inside dynamics of pulled and pushed fronts. *J. Math. Pures Appl.* (9) 98, no. 4, 428-449 (2012).

8. J. Garnier and M. A. Lewis, Expansion under climate change: the genetic consequences. *Bull. Math. Biol.* 78, no. 11, 2165-2185 (2016).
9. S.-B. Hsu and X.-Q. Zhao, Spreading speeds and traveling waves for nonmonotone integrodifference equations. *SIAM J. Math. Anal.* 40, no. 2, 776-789 (2008).
10. H. Inaba, Mathematical analysis of an age-structured SIR epidemic model with vertical transmission, *Discrete Contin. Dyn. Syst. Ser. B*, 6, 69-96 (2006).
11. M. Kot, M.A. Lewis and P. van den Driessche, Dispersal data and the spread of invading organisms, *Ecology*, 77 (7), 2027-2042 (1996).
12. M. G. Kreĭn and M. A. Rutman, Linear operators leaving invariant a cone in a Banach space. *Uspehi Matem. Nauk (N. S.)* 3 no. 1 (23), 3-95 (1948).
13. M. A. Lewis, Variability, patchiness, and jump dispersal in the spread of an invading population. In: D. Tilman, P. Kareiva (eds.) *Spatial Ecology: The Role of Space in Population Dynamics and Interspecific Interactions*, pp. 4669. Princeton University Press, Princeton, NJ (1997).
14. T. Leinster and C. A. Cobbold, Measuring diversity: the importance of species similarity, *Ecology*, 93 (3), 4770489 (2012).
15. R. Lui, A nonlinear integral operator arising from a model in population genetics. I. Monotone initial data. *SIAM J. Math. Anal.* 13, no. 6, 913-937 (1982).
16. R. Lui, A nonlinear integral operator arising from a model in population genetics. II. Initial data with compact support. *SIAM J. Math. Anal.* 13, no. 6, 938-953 (1982).
17. R. Lui, Existence and stability of travelling wave solutions of a nonlinear integral operator. *J. Math. Biol.* 16, no. 3, 199-220 (1982/83).
18. R. Lui, A nonlinear integral operator arising from a model in population genetics. III. Heterozygote inferior case. *SIAM J. Math. Anal.* 16, no. 6, 1180-1206 (1985).
19. B. Li, M. A. Lewis and H. F. Weinberger, Existence of traveling waves for integral recursions with nonmonotone growth functions. *J. Math. Biol.* 58, no. 3, 323-338 (2009).
20. N. G. Marculis, R. Lui and M. A. Lewis, Neutral genetic patterns for expanding populations with nonoverlapping generations. *Bull. Math. Biol.* 79, no. 4, 828-852 (2017).
21. I. Marek. Frobenius theory of positive operators: comparison theorems and applications, *SIAM J. Appl. Math.*, 19, 607-628 (1970).
22. L. Roques, J. Garnier, F. Hamel and E. K. Klein, Allee effect promotes diversity in traveling waves of colonization. *Proc. Natl. Acad. Sci. USA* 109, no. 23, 8828-8833 (2012).
23. C. Parmesan, Climate and species' range. *Nature* 382, 6594, 765 (1996).
24. S. U. Pauls, C. Nowak, M. Bálint, and M. Pfenninger. The impact of global climate change on genetic diversity within populations and species. *Molecular ecology*, 22(4), 925-946 (2013).
25. A. B. Potapov and M. A. Lewis, Climate and competition: the effect of moving range boundaries on habitat invasibility. *Bull. Math. Biol.* 66 (2004), no. 5, 975-1008.
26. J. Powell, Spatio-temporal models in ecology; an introduction to integrodifference equations, (2001).
27. I. Sawashima, On spectral properties of some positive operators, *Nat. Sci. Report Ochanomizu Univ.*, 15, 53-64 (1964).
28. E. H. Simpson, Measurement of diversity, *Nature*, 163, 688 (1949).
29. C. E. Shannon, A mathematical theory of communication. *The Bell System Technical Journal*, 27, 379423 (1948).
30. P. Takáč, A short elementary proof of the Kreĭn-Rutman theorem. *Houston J. Math.* 20, no. 1, 93-98 (1994).
31. H. F. Weinberger, Long-time behavior of a class of biological models. *SIAM J. Math. Anal.* 13, no. 3, 353-396 (1982).
32. X.-Q. Zhao, Global attractivity and stability in some monotone discrete dynamical systems. *Bull. Austral. Math. Soc.* 53, no. 2, 305-324 (1996).
33. Y. Zhou and M. Kot. Discrete-time growth-dispersal models with shifting species ranges. *Theoretical Ecology* 4, 1, 13-25 (2011).